A TRANSFERRIN CONJUGATED NANOEMULSION SYSTEM FOR BRAIN DELIVERY OF ANTIRETROVIRAL THERAPY

A Dissertation
Submitted to
the Temple University Graduate Board

In Partial Fulfillment
of the Requirements for the Degree
DOCTOR OF PHILOSOPHY

---

by
Mengjie Si
May 2019

Examining Committee Members:

Ho-lun Wong, Advisory Chair, Pharmaceutical Science, School of Pharmacy
Daniel J. Canney, Pharmaceutical Science, School of Pharmacy
Reza Fassihi, Pharmaceutical Science, School of Pharmacy
Haifeng Cui, External Examiner, Scientific Director, Senior Fellow, GlaxoSmithKline

ABSTRACT

HIV- associated neurocognitive disorder (HAND), also known as HIV encephalopathy and AIDS dementia, is one of the critical complications of HIV infection that causes severe morbidity and even shortens survival. This complication is challenging to treat because most of the antiretroviral therapeutic (ART) agents cannot achieve the desired therapeutic levels in the central nervous system (CNS) because they cannot efficiently cross the blood-brain barrier (BBB). The goal of this study is to develop a new transferrin conjugated nanoemulsion system (Tf-NE) for antiretroviral medication delivery and evaluate its potential to cross the BBB.

Nanoemulsions were prepared based on the solvent evaporation sonication method using lipids and phospholipids. To achieve brain delivery, holo-transferrin was conjugated to DSPE-PEG (2000)-Maleimide by NHS ester crosslinking reaction. Darunavir (DRV) was encapsulated into Tf-NE as an antiretroviral agent. Size, polydispersity index, and dispersion stability were characterized using dynamic light scattering (DLS) system. Morphology of the Tf-NE was investigated using transmission electron microscopy (TEM). Differential scanning calorimetry was performed to study the extent of drug solubilization inside the nanoemulsion system. To evaluate the in vitro toxicity of Tf-NE-DRV, MTT assay was performed by using the human brain endothelial capillary hCMEC/D3 cells and 293T cells. Cell uptake and drug transport assays were also conducted to investigate the in vitro activity of Tf-NE-DRV. In vitro efficacy studies, ex vivo imaging studies and in vivo biodistribution studies were performed to investigate the brain targeting function of Tf-NE-DRV.

Tf-NE-DRN was prepared 100-130nm in diameter with polydispersity index smaller than 0.3. This nanoemulsion system was stable in serum-enriched medium and water at 37 ℃ for 5 days. All the therapeutic compounds were well-dispersed inside the oil core of Tf-NE-DRV. Within the therapeutic concentration range, Tf-NE-DRV did not cause a significant reduction in the cell viability, indicating low toxicity of the formulation. Considerable uptake of Tf-NE-DRV into the BBB model of hCMEC/D3 cells was observed. Tf-NE-DRV can maintain the same therapeutic function as the free drug form of darunavir in vitro. Imaging and biodistribution results revealed the formulation was superior to the free drug and able to transport the drug across the BBB in vivo to reach the therapeutic level.

We successfully developed a biocompatible nanoemulsion system that can effectively penetrate the BBB. This Tf-NE-DRV system shows the clinical potential to deliver antiretroviral agents into the CNS system to achieve improved treatment of HAND.

THIS DISSERTATION IS DEDICATED TO

MY PARENTS, ZHIJUN SI & YONGHONG XU

MY HUSBAND, HANGHANG ZHANG

ACKNOWLEDGMENTS

Firstly, I would like to thank my advisor Dr. Ho-lun Wong. I knew nothing about nanoparticle when I joined his lab at first. He is always willing to help and is supportive of our studies, researches as well as our lives. He creates such a free and flexible environment in our lab so that we can grow and develop into the way we want. I appreciate all the guidance and advice from him, which benefits my life and work.

I would also like to thank my committee members Dr. Dianel J. Canney and Dr. Reza Fassihi. Thank you for all the support throughout my study and good advice towards my research.

I'd like to thank Dr. Marc Ilies for granting me access to all the instruments like DSL, DSC, and NMR. I appreciate all the training and instruction from the students in Dr. Illies' lab. I'd like to thank John C. Gordon for helping me with the biodistribution studies. I'd like to thank Dr. Wenhui Hu and his student on helping me with the in vitro disease model establishment and in-vitro anti-HIV efficiency study.

I feel grateful to have all my lab members. They are all outstanding teachers to me, and I learned a lot from them. Thank them for all the help they have provided.

I'd like to thank Temple School of Pharmacy for accepting me into this Ph.D. Program. Without their help and financial support, I won't be able to finish my Ph.D. study, and you won't be able to see this thesis.

Last but not least, I’d like to thank my beloved parents and my husband. They are the reason why I’m here. They are always so encouraged and supportive. I won’t be able to achieve this without them.

TABLE OF CONTENTS

LIST OF TABLES

LIST OF FIGURES

ABBREVIATION

Acquired Immune Deficiency Syndrome	AIDS
Azidothymidine	AZT
Absorptive-mediated transcytosis	AMT
Blood-Brain Barrier	BBB
Combination antiretroviral therapy	cART
Central Nervous System	CNS
Critical micelle concentration	CMC
Carrier-mediated transcytosis	CMT
CNS penetration effectiveness	CPE
Cell-penetrating peptide	CPP
Cerebrospinal fluid	CSF
1,2-distearoyl-sn-glycero-3-phosphocholine	DSPC
1,2-distearoyl-sn-glycero-3-phosphoethanolamine-N-[methoxy(polyethylene glycol)-2000] (ammonium salt)	DSPE
Docosahexaenoic acid	DHA
fluorescein isothiocyanate	FITC
Human immunodeficiency virus	HIV
HIV-Associated Neurocognitive Disorder	HAND
Low-density lipoprotein	LDL
Nucleoside reverse transcriptase inhibitors	NRTI
Non-nucleoside reverse transcriptase inhibitors	NNRTI
Protease inhibitors	PI
Poly (ethylene glycol)	PEG
Poly (lactic acid)	PLA

Poly (D, L-Lactic-co-glycolide)	PLG
Ultrasound-mediated drug delivery	UMDD
Reticuloendothelial system	RES
Receptor-mediated transcytosis	RMT
Transferrin	Tf
Transferrin receptor	TfR
Trans-activating transcriptor	TAT
N-succinimidyl S-acetylthioacetate	SATA
4-(2-hydroxyethyl)-1-piperazineethanesulfonic acid	HEPES
Ethylenediaminetetraacetic acid	EDTA
Nanoemulsion	NE
Phosphate-buffered saline	PBS
Polyethylene terephthalate	PET
Dimethyl sulfoxide	DMSO
Differential scanning calorimetry	DSC
Polydispersity index	PDI

CHAPTER 1

INTRODUCTION

1.1. Lipid nanotechnology platforms for drug delivery

The development of nanoparticle-based drug formulation has yielded opportunities to address and treat challenging diseases. Nanoparticles vary in size but are generally from 10 to 500nm. Through the manipulation of size, surface characteristics and material components, the nanoparticle can be developed into smart systems, which can carry therapeutic agents and imaging agents as well as bearing stealth property. Further, these systems can deliver the drug to specific tissues and provide controlled release therapy. This targeted and sustained drug delivery decreases the related drug toxicity and increases patients' compliance with less frequent dosing. Nanotechnology has proven beneficial in the treatment of cancer, AIDS and other diseases, also providing advancement in diagnostic testing. [1]Lipid nanoparticle drug delivery research is mainly focused on a few popular platforms as shown in Figure 1.1, and we will discuss them one by one.

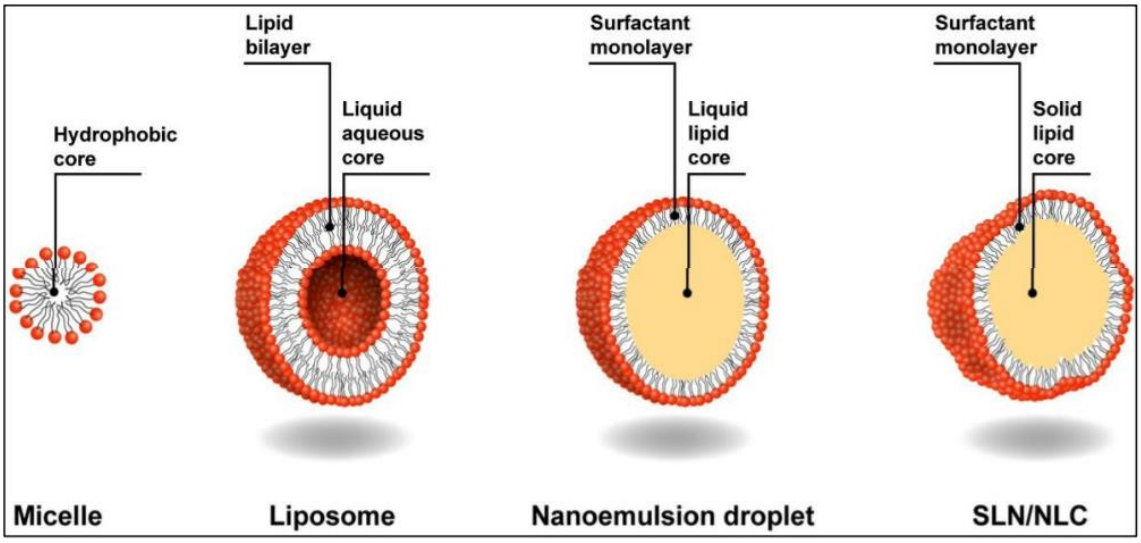

Figure 1.1 Comparison between micelles, liposomes, nanoemulsions and solid lipid nanoparticles[2].

1.1.1. Liposome

Liposomes are small vesicles comprised of one or more phospholipid bilayers enclosing an aqueous core. In addition to their low toxicity and ability to deliver both hydrophilic and lipophilic compounds, the liposome is the most well-studied and clinically recognized nanoparticle, which was developed early in the 70's. Their size, surface charge, lipid composition can be manipulated to control drug delivery and tissue uptake.

The most common liposomal formulations in targeting the BBB are cationic, PEGylated and immunoliposomes[3]. Although the mechanism is not entirely understood, it is suggested that the cationic liposomes bind to the negatively charged endothelium of the brain and due to their small size (20nm), they can then be transported via passive diffusion or phagocytosis[4]. PEG-grafted on the surface of liposomes enables them to evade the Reticuloendothelial (RES) system. Therefore, lengthening their blood circulation time and giving them time to slip past the BBB. Without PEG, liposomes tend to either be engulfed by phagocytes or exchange lipid materials with cell membranes[5]. As with many other nanoparticle formulations, liposomes can also be complexed with an antibody or ligand that will be recognized by a BBB receptor, inducing receptor-mediated endocytosis. PEGylated liposomes around 100nm in diameter functionalized with transferrin and loaded with horseradish peroxidase were used in vitro to deliver the drug to the lysosomes of brain endothelial cells[6].

1.1.2. Nanoemulsion (NE)

Nanoemulsions are kinetically stable liquid-in-liquid dispersions with droplet sizes on the order of 100nm. A typical nanoemulsion contains oil, water, and an emulsifier. The addition of an emulsifier is critical for the creation of small size droplets as it decreases the interfacial tension. The emulsifier also plays a role in stabilizing nanoemulsions through repulsive electrostatic interactions and steric hindrance.[7] The emulsifier used is generally a surfactant, but proteins and lipids have also been useful in the preparation of nanoemulsions.[8, 9]

Nanoemulsions have been used in most forms of drug delivery, namely topical, ocular, intravenous, internasal and oral delivery. These applications leverage the lipophilic nature of nanoemulsions to formulate aqueous solutions which can efficiently be delivered to the patient.

1.1.3. Solid lipid nanoparticle (SLN)

Solid lipid nanoparticles comprise a solid hydrophobic core of lipids, such as mono-, di- and triglycerides or fatty acids with a monolayer of phospholipid structure. They are surfactant stabilized lipid oily droplet, which is generally solid at room temperature. Like polymeric nanoparticles, they are capable of controlled release of up to several weeks and can also be coated or grafted with ligands for drug targeting[10]. Solid lipid nanoparticles are stable as well as biodegradable under physiological conditions[11]. Thus, it is an attractive alternative to liposomes and polymeric nanoparticles. Due to its lipophilic center, this technique is more suitable for lipophilic drugs as well as peptides and proteins[1].

1.1.4. Polymeric nanoparticle

Polymeric nanoparticles are a particulate dispersion of biodegradable and biocompatible polymers with size 10-1000nm[12]. The core of these polymeric nanoparticles made up of a dense polymer matrix to encapsulate the hydrophobic drug and hydrophilic polymers inside the structure to serve steric stability and stealth properties to nanoparticle[13]. The most common polymers for controlled drug release applications today are poly(lactic acid) (PLA), poly(aspartic acid), poly(butyl cyanoacrylate) (PBCA), poly(glycolic acid)

(PGA), poly(D,L-lactic-co-glycolide) (PLGA), with PLA, PGA and PLGA being the most extensively used in CNS drug delivery[14]. Availability of polymer choice and drug release from nanoparticle makes them unique candidates for drug delivery. Level of drug release is not only controlled by molecular weight and polymer composition, but the drug-to-polymer ratio also affects[15]. The role of polymeric nanoparticles in drug delivery can be considered non-replaceable considering its broad application and excellence[16-18].

1.1.5. Micelle

Micelles are monolayered spherical lipid nanostructures with inwards facing hydrophobic ends and outwards facing hydrophilic ends with a range of 80 – 100nm[19]. Due to its small size, the micelles shows short circulation time in the body compares to liposomes that make them easily transportable elements[20]. Polymeric micelles considered as more stable with longevity and good biodistribution compare to traditional micelles. These modified micelle shows improved target penetration due to their nanoscale size, easy transportation to the target location, and low critical concentration (CMC)[21]. Physically entrapped and covalently bonded micelles drug conjugate play an essential role in controlled drug release system[22]. Drug loading to micelles generally depends on upon the physiological property of drug, the chemical composition of the core forming polymers, and physical state of micelles core[23]. The release is generally affected by temperature, pH, and environment[24].

1.1.6. Summary

After comparing all the characteristics of the different category of nanoparticle platforms, we decided to utilize the nanoemulsion system for our project. The drug we are trying to deliver is a lipophilic drug while the nanoemulsion system explicitly offers the potential to deliver high concentrations of oil-soluble compounds. The lipophilic drug can disperse evenly inside the oil core, and the drug release profile will be sustained and smooth. Since we are trying to achieve CNS delivery, we try to use all natural materials to make our drug delivery systems. Nanoemulsion systems are the only one which complies with all these requirements.

	Macroemulsions	Nanoemulsions	Microemulsions
Size	1-100um	20-500nm	10-100nm
Shape	Spherical	Spherical	Spherical, lamellar
Stability	Thermodynamically unstable, weakly kinetically stable	Thermodynamically unstable, kinetically stable	Thermodynamically stable
Appearance	Turbid	Transparent	Transparent
Method of preparation	High & low energy methods	High & low energy methods	Low energy methods
Polydispersity	Often high (>40%)	Typically low (<10-20%)	Typically low (<10%)

Table 1.1 Comparison of Macroeulsions, nanoemulsions, and microemulsions with respect to size, shape, stability, appearance, a method of preparation, and polydispersity. Nanoemulsions and microemulsions have a larger surface area per unit volume than macroemulsions because of their size. In addition, due to a strong kinetic stability, nanoemulsions are less sensitive to physical and chemical changes.

1.2. Method of nanoemulsion preparation

Over the past decade or more, the research focus has been on preparing nanoemulsions through various ways, broadly classified into two primary categories: high-energy and low energy methods.[25, 26] High energy methods such as high-pressure homogenization (HPH) and ultrasonic emulsification consume significant energy (~ 10^8 - 10^{10} W kg^{-1}) to make small droplets. On the other hand, low energy methods exploit specific system properties to make small droplets without consuming significant energy (~ 10^3 W kg^{-1}). Production of nanoemulsion is achieved by using the intrinsic physiological properties of the system. Phase inversion temperature (PIT)[25] and emulsion inversion point (EIP)[27] are two examples of low energy approaches for the formation of nanoemulsions. At the initial studies of nanoemulsion, the high energy methods were only choice for researchers.[28] Nowadays, low energy methods have drawn considerable attention since they are 'soft', non destructive and cause no damage to encapsulated molecules.[29] Recently, a few novel technologies such as bubble bursting at oil/water interface[30] and evaporative ripening[31] have also been developed for making nanoemulsions.

1.2.1. High-pressure homogenization (HPH) method

High-pressure homogenization method is the most popular one used for nanoemulsion production. This method benefits from the piston homogenizer (Figure 1.2) to manufacture nanoemulsion that particle sizes up to 1 nm. Extremely small droplet sized nanoemulsions are achieved because during the process several forces like hydraulic shear, intense turbulence and cavitation act together. This process can be repeated until the final product reaches the desired droplet size and polydispersity index(PDI).[32] The

uniformity of droplet size is measured by PDI. A large amount of energy and increasing temperature during process might cause deterioration of the components.[33]

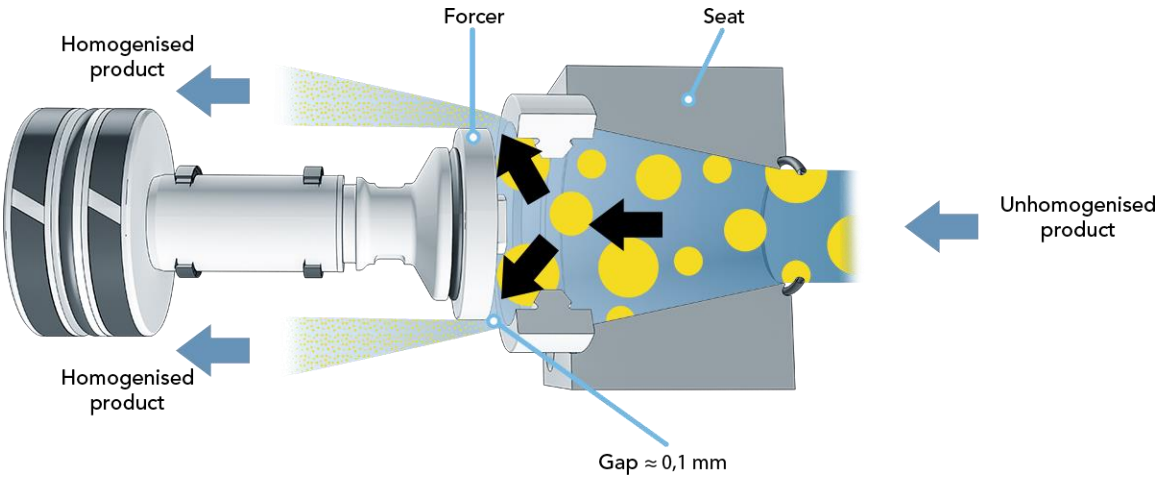

Figure 1.2 Schematic representation of Piston homogenizer

1.2.2. High shear stirring method

In this method, high-energy mixers and rotor-stator systems are used for the preparation of nanoemulsions. Droplet sizes of the internal phase can be significantly decreased by

increasing the mixing intensity of these devices. However, obtaining an emulsion with the average droplet size less than 200-300nm is rather difficult.[28]

1.2.3. Ultrasonic emulsification method

There are mainly two mechanisms taking part in this method. Firstly, the acoustic field creates interfacial waves that make the oil phase to disperse in the continuous phase as droplets. Secondly, ultrasound provokes acoustic cavitation which provides formation and collapse of microbubbles respectively due to pressure fluctuations of a single sound wave. In this way, enormous levels of highly localized turbulence are generated, and this causes micro implosions which disrupt large droplets into sub-micron size.[34 35]

1.2.4. Microfluidization method

This is the most widely employed in the pharmaceutical industry in order to acquire fine emulsions. In this method, a device called microfluidizer (Figure 1.3) is used which provides high-pressure force to break the droplets. Uniform nanoemulsion production can be achieved by repeating this process.[36]

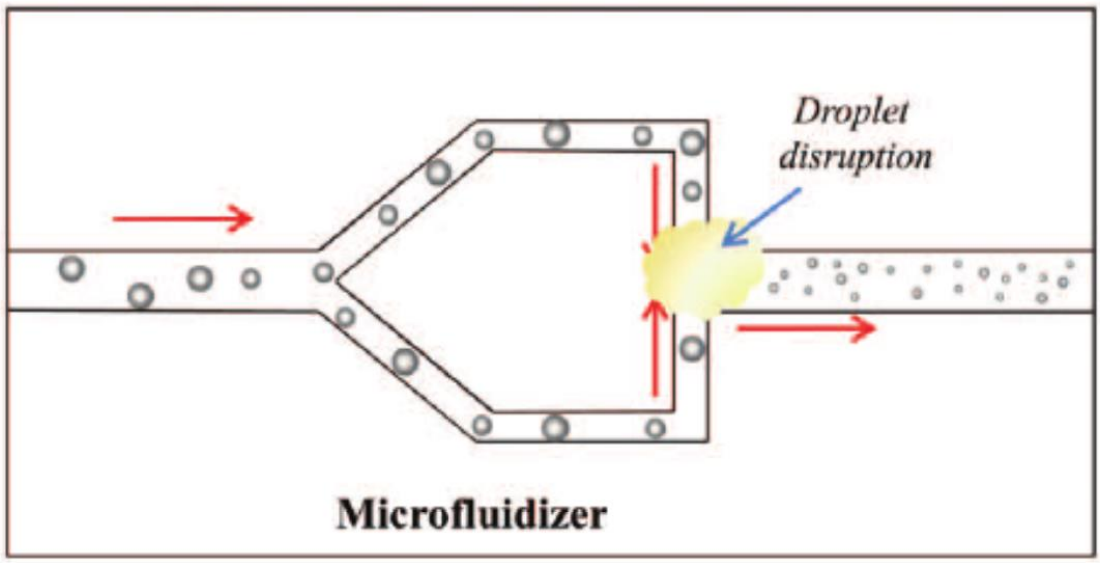

Figure 1.3 Schematic representation of microfluidizer

1.3. HIV infection and HIV-associated neurocognitive disorder (HAND)

1.3.1. The epidemic of HIV infection

The infection caused by the human immunodeficiency virus (HIV), will develop into acquired immune deficiency syndrome (AIDS) with the human immunodeficiency virus over time. There are three main stages of HIV infection: acute infection, chronic infection, and AIDS, which is defined regarding either a CD4+ T cell count below 200 cells per uL or the occurrence of specific diseases in association with an HIV infection[37]. Acute HIV infection is the earliest stage of HIV infection, and it generally develops within 2 to 4 weeks after infection with HIV. In the acute stage of infection, HIV multiplies rapidly and spreads throughout the body. The virus attacks and destroys the

infection-fighting CD4 cells of the immune system. During the acute HIV infection stage, the level of HIV in the blood is very high, which greatly increases the risk of HIV transmission. The second stage of HIV infection is chronic HIV infection (also called asymptomatic HIV infection or clinical latency). During this stage of the disease, HIV continues to multiply in the body but at very low levels. People with chronic HIV infection may not have any HIV-related symptoms, but they can still spread HIV to others. Without treatment with HIV medicines, chronic HIV infection usually advances to AIDS in 10 years or longer, though in some people it may advance faster. AIDS is the final, most severe stage of HIV infection. Because HIV has severely damaged the immune system, the body can't fight off opportunistic infections. Opportunistic infections are infections and infection-related cancers that occur more frequently or are more severe in people with weakened immune systems than in people with healthy immune systems.

According to the data from the U.S. Department of Health & Human Services, about thirty-seven million people are living with AIDS in 2015 worldwide. The same year estimated 2.1 million individuals worldwide were newly infected. An estimated 35 million people have died from AIDS-related illnesses since the start of the epidemic, including 1.1 million in 2015. In the absence of specific treatment, around half of people infected with HIV develop AIDS within ten years[38]. Without treatment, people who progress to AIDS typically survive for about three years. Once you have a dangerous opportunistic illness, life- expectancy without treatment falls to about one year[37]. Thanks to the introduction of antiretroviral therapy, HIV infection has been transformed from a

terminal disease to a chronic, yet manageable condition and has significantly reduced HIV related mortality[39]

1.3.2. Introduction of antiretroviral and HIV treatment

HIV is a type of virus called retrovirus, and the drugs used to treat it are called antiretroviral drugs. Although there is no cure or effective HIV vaccine on the market, highly active antiretroviral therapy has successfully slowed the progression of the disease. There are six main classes of antiretroviral drugs: (1) Nucleoside reverse transcriptase inhibitors (NRTIs), (2) Non-nucleoside reverse transcriptase inhibitors (NNRTIs), (3) Protease inhibitors (Pis), (4) Integrase inhibitors, (5) Fusion inhibitors and (6) Chemokine receptor antagonists (CCR5 antagonists). They are grouped into different classes according to how they fight HIV, and each class of the antiretroviral drugs targets a different stage of the HIV life cycle (Fig 4). There are seven stages of the HIV life cycle: (1) binding, (2) fusion, (3) reverse transcription, (4) integration, (5) replication, (6) assembly and (7) budding.

The limitations of single-drug treatment regiments quickly became apparent. HIV replicates swiftly and is prone to errors each time it does. These errors, or mutations, cause small changes in the virus. HIV variants with mutations that confer resistance to an antiretroviral drug can evolve rapidly. In some people taking azidothymidine(AZT) which is the first drug treating HIV infection, drug resistance developed in a matter of days. In the early 1990s, scientists found that AZT in combination with ddC showed more effective outcome than AZT alone, and it is the first introduction of the

combination antiretroviral therapy (NIH, HIV/AIDS treatment). Nowadays, combinational (also known as “cocktail”) antiretroviral therapy has become the standard treatment of HIV infection, which combines drugs from at least two different classes. This standard therapy could durably suppress HIV replication to minimal levels, which creates a high genetic barrier against the development of drug resistance.

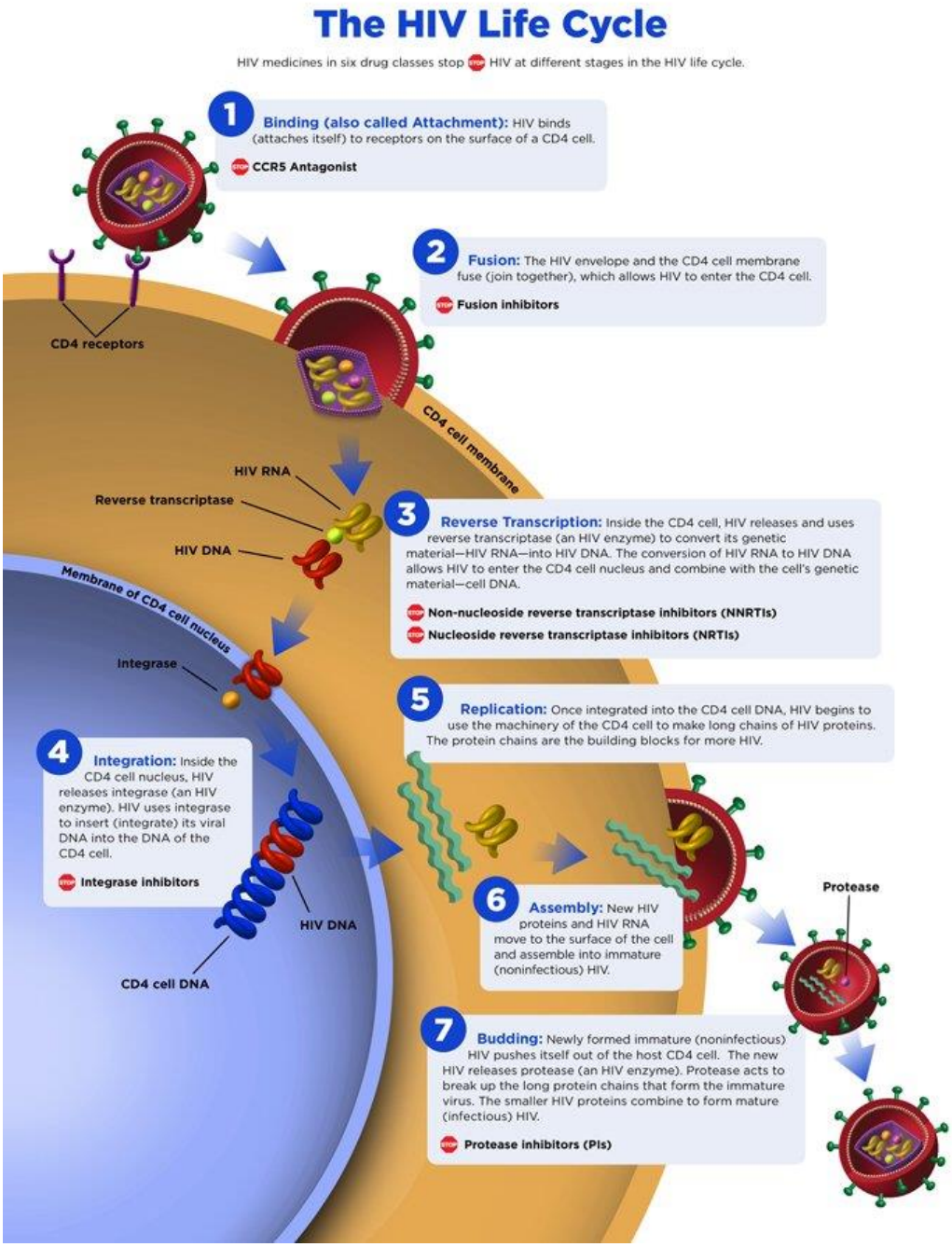

Figure 1.4 HIV life cycle and how are different classes of antiretroviral drugs fight HIV.

(AIDS info, US department of health and human service, https://aidsinfo.nih.gov)

1.3.3. Pathophysiology of HIV

When immune defenses are impaired, opportunistic infections and neoplasms arise, often from reactivation of previously acquired organisms. This mechanism applies to agents such as Toxoplasma gondii and Epstein-Barr virus (EBV); the latter is strongly associated with CNS lymphoma. Other organisms, such as the JC or SV40 viruses that cause PML, may be activated directly by HIV gene products.

The likelihood of a particular neurologic syndrome correlates with the clinical stage of HIV infection as reflected by viral load, immune response, and CD4+ lymphocyte counts. This, in turn, is related to the severity of immunodeficiency and autoimmunity and to serum and tissue cytokine levels.

The entrance of HIV into the CNS occurs early in the course of infection, likely within days to weeks. In contrast to the periphery where HIV infects the CD4+ T cells, in the brain, HIV targets astrocytes and perivascular macrophages/microglial cells. Several mechanisms of entry have been proposed and likely relates to transendothelial migration of infected CD4 lymphocytes and/or migration of infected monocytes.[40, 41]

Replication of HIV in the CNS results in the stimulation of proinflammatory cytokines and neurotoxins, leading to oxidative stress. Macrophages infected with the virus can form multinucleated giant cells, a classic feature seen on the pathology of HIV infection in the brain. Astrocytes act as a reservoir for the virus, which typically is dormant there unless the host cells contact lymphocytes or become activated by cytokines. Due to the

slow turnover rate of astrocytes, this site allows the virus to reside in the brain indefinitely, thereby rendering its eradication unsuccessful thus far.

Neurons are not directly infected with the virus and damage ensues through indirect processes such as neurotoxic proteins Tat and GP120 or through the release of proinflammatory cytokines from infected macrophages. Areas of the brain most vulnerable to damage include but are not limited to the basal ganglia, subcortical white matter, and frontal cortex.

1.3.4. HIV-associated neurocognitive disorder (HAND)

In the early days of the HIV epidemic, the literature was rich with accounts of patients with advanced AIDS presenting with accelerated dementia who progressed from apathy, reduced concentration and impaired short-term memory to global dementia, loss of motor function and incontinence in the span of months[42]. These cerebral manifestations of HIV infection with the disturbance of cognitive, behavioral, motor, and autonomous functions remain an issue in the everyday practice of HIV medicine[43]. The older terms of HIV encephalopathy and AIDS dementia complex have been replaced by the term HIV-associated neurocognitive disorder (HAND)[44].

The incidence of HAND was found to be less decreasing than that of the other AIDS-defining conditions — patients who were diagnosed and treated early after infection had a low prevalence of neurocognitive impairment[45].The HAND is associated with shortened survival[46]. During primary infection, HIV enters the brain parenchyma via

infected lymphocytes and monocytes and probably by trans ependymal migration[47]. This is the reason why inflammatory CSF changes are already present in the asymptomatic stages of the infection in almost all individuals[48, 49]. The basal ganglia and the frontal white matter are the earliest and most intensely affected brain regions[50]. The cellular basis of carriage and production of the virus are the immunocompetent cells such as perivascular microglia and lymphocytes[51]. Neurons, astrocytes, and oligodendroglia are not or only minimally infected. They are, however, affected as evidenced by loss of synapses and neuros[47, 52], by apoptosis as well as by the production of osteopontin, a pro-inflammatory cytokine[53]. Many studies have found a positive correlation between the amount of virus and viral products and the extent of histopathologic changes in the brain[54, 55]. In addition, the grade of clinical neurologic dysfunction is related to the degree of macrophage activation on histopathology[54, 56, 57]. A higher CNS viral load predicts the future development of HAND[58].While in the pre-cART era, the CD4 cell count and the plasma viral load predicted the progress of HAND, this is no truer for the cART era. In addition, the HAND does now occur in earlier stages of the HIV infection[59].

The hypothesis that HIV-associated dementia was due to neurotoxic effects of HIV itself, and not due to opportunistic infections, was already established in the mid-1980s[60]. Significant neuropathological damage occurs in the course of HIV infections of CNS, leading to severe neurological manefestations[39]. It has previously been postulated a long time ago that " effective specific antiviral therapy would have to possess the capacity to penetrated the blood-brain barrier[61]." With the assumption that the HIV infection of the brain is the prerequisite for the development of HAND, the mainstay of a causal

treatment is the suppression of virus replication in the brain. Early treatment with greater CNS activity, and ensuring adherence, appear to confer benefit in neuropsychiatric performance, improve function and quality of life, and improve all-around morbidity in HIV-infected individuals[62].

HIV is now becoming one of the leading causes of dementia worldwide along with Alzheimer's disease and vascular dementia. HIV is also now becoming one of the leading causes of neuropathy worldwide, along with diabetes and leprosy. [63]

cART leads to a lower virus load in the brain parenchyma as well as in the CSF. There is an improvement of electrophysiological parameters and, finally, a randomized clinical study has demonstrated improved cognitive function[64-67]. Notable improvement starts some 4 – 8 months after the start of treatment[68].The degree of clinical improvement is higher in more severely affected patients, and it corresponds to the increase of CD4-lymphocytes[59, 69]. For the detection of CSF virus, an ultrasensitive PCR technique detecting down to 2 copies per ml CSF might be employed, as low-level virus replication was shown to be associated with neurocognitive impairment[70].

A CNS penetration effectiveness score (CPE), composed of the relative values of CNS penetration of the substances in a given cART regimen, has been devised by Letendre[71]. It comprises four categories, where lower scores indicate lower CNS penetration (Table 3). Several authors worked on the impact of the CNS penetration on the CSF viral load and cognitive, clinical endpoints. Most studies showed higher CPE scores to be

associated with lower CSF viral load[72-74]. For the treatment of HAND, CNS-penetrating substances should be considered.

1.3.5. Challenges for CNS delivery of antiretroviral therapy

The CNS is a site that ART often has difficulty reaching. The presence of BBB, blood-cerebrospinal fluid barrier (BCSFB), efflux transport systems and high expression of metabolizing enzymes, hinders the free entry of majority of ARV drugs to the brain, thus making eradication of HIV from the CNS an alarming task, in spite of marked advances in cART. BBB is a complex interface between bloodstream and brain parenchyma and is composed of three cellular components of the brain microvasculature, namely, endothelial cells, pericytes, and astrocyte endfeet processes[75, 76]. The endothelial cells of the brain is different from its peripheral counterpart in that it is connected together by tight junctions with a tightness of about 50–100 folds higher than the other and has a very high electrical resistance of about 1500–2000 Xcm^2. The BBB shows unique biological characteristics such as: lack of fenestrations, very few pinocytic vesicles and a very high mitochondrial content[77, 78]. All these distinctive features of BBB restrict the passage of ARVs from blood to the brain. Other than that, certain anti-HIV drugs including protease inhibitors were demonstrated to have greater CNS efflux than influx, suggesting the involvement of efflux transporters like P-glycoprotein present in the BBB[79-81]. This further allows the virus to reside inside the CNS and seed the entire body without any difficulty, as the virus is relatively protected from the immune system by the BBB, increasing the chance of a viral mutation leading to drug resistance.[82]

Table 1.2 Central nervous system penetration-effectiveness ranking

Drug Class	CPE Score			
	4	**3**	**2**	**1**
Nucleoside Reverse Transcriptase Inhibitors	Zidovudine	Abacavir Emtricitabine	Didanosine Lamivudine Stavudine	Tenofovir Zalcitabine
Nonnucleoside Reverse Transcriptase Inhibitors	Nevirapine	Delavirdine Efavirenz	Etravirine	
Protease Inhibitors	Indinavir/r	Darunavir/r Fosamprenavir/r Indinavir Lopinavir/r	Atazanavir Atazanavir/r Fosamprenavir	Nelfinavir Ritonavir Saquinavir Saquinavir/r Tipranavir/r
Entry/Fusion Inhibitors		Maraviroc		Enfuvirtide
Integrase Strand Transfer Inhibitors		Raltegravir		

Due to the ineffectiveness of existing therapies in the delivery of anti-HIV drugs to the CNS, research has been directed towards the development of new strategies for effective delivery of drugs to the brain for the treatment of CNS infection of HIV[39].

1.4. Strategies for CNS drug delivery

1.4.1. Disruption of the BBB

To increase the permeability of BBB, techniques have been developed to disrupt the endothelial cells temporarily, allowing macromolecular drugs to leak into the CNS[83]. One technology uses an osmotic shock to shrink the endothelial cells and disrupt the tight junctions. In a clinical study, the disruption followed by the subsequent administration of chemotherapeutic agents allowed sufficient drug molecules to cross the BBB in order to produce a therapeutic effect in brain cancer patients[84]. More recently, ultrasound-mediated drug delivery (USMD) that uses microbubbles that are 1-10 um in diameter to mechanically disrupt the tight junctions is showing potential for enhanced chemotherapy treatment especially regarding spatial specificity, as ultrasound waves can be targeted within an area of a few millimeters[85-87]. USMD is of high clinical relevance as various chemotherapy drugs as well as other therapeutic agents have been successfully transported across the BBB via this approach[88]. Recent studies tested the technology on primates and found that the ultrasound-induced BBB opening in the basal ganglia did not result in any visual or motor deficits[89]. However, although USMD shows promise in animal models, potential limitations still include the narrow sonication field and the targeting aberrations due to the skull; thus, further studies need to be done to confirm its clinical potential in humans.

1.4.2. Direct injection into CNS

Transcranial injections, either intracerebrally or intracerebroventricularly, offer the most direct delivery of drug to the tumor site, thus reducing possible adverse effects on peripheral healthy tissue. Alternatively, a biodegradable chemotherapeutic impregnated wafer, such as the Gliadel wafer, can be implanted into the tumor resection cavity. Both approaches above rely on diffusion to transport the drug into the brain parenchyma. However, as diffusion in the brain decreases exponentially with distance, this technology has significant limitations and requires precise mapping of the injection or implantation site to achieve maximum targeting of the drug to the tumor[90].

1.4.3. The major problem of invasive delivery

Unfortunately, like any invasive technique, the methods mentioned before are companied by a high neurosurgical cost and increased risk of infection as undesirable elements may enter the brain when the BBB is exposed. The brain could suffer as well from various traumatic injuries due to the mechanical nature of these approaches.

1.4.4. Prodrugs

Drugs that can cross the BBB via passive diffusion have the following common characteristics: 1) small molecular size of less than 500Da 2) high lipophilicity and 3) lack of ionization at physiological pH. Thus, there is much effort directed towards making water-soluble drugs lipid-soluble by reducing the number of its polar groups or by linking them to lipid moieties. However, this engineering challenge is significant, and until now, no drug modified in this manner has been able to cross the BBB in

pharmacologically substantial amounts, with the one exception being the acetylation of morphine to form heroin[91, 92].

Apart from the passive diffusion route, other transport mechanisms, such as carrier-mediated or receptor-mediated transport have been exploited to more success in trafficking prodrugs across the BBB.

1.4.5. Intranasal drug delivery

Intranasal drug delivery is a non-invasive drug delivery technique that bypasses the BBB via the olfactory nerves[93]. Recent studies have revealed its potential for possible treatment of autism spectrum disorder, as intranasal oxytocin improved social and emotional functioning in autistic individuals[94]. The ease and safety of administration of methotrexate to brain tumors reduced brain tumor weight by 80%[95]. However, the primary limitation is the small number of molecules capable of diffusing through the olfactory epithelium[83].

1.4.6. Nanomedicine for CNS drug delivery

Nanoparticles are gaining broad interest as carriers for CNS delivery of various therapeutic agents[96]. This is because nanoparticles offer more stability to the encapsulated drug in biological fluids and against enzymatic metabolism as compared to other colloidal systems, such as liposomes or micelles[97]. There are a few basic essential criteria that need to be carefully considered in designing such drug delivery devices across the BBB. Firstly, these nanocarriers loaded with therapeutic drugs often should have a small size. It may be necessary to control the size to be around 100nm to achieve efficient

transport across BBB and diffusion within the brain parenchyma[98, 99]. Secondly, the surface of the nanocarriers has to be sufficiently hydrophilic in order to minimize the adsorption of opsonins. A conventional technique to avoid opsonins is to incorporate poly (ethylene glycol) (PEG) – containing compounds into the nano particulate system to create a surface water-bound layer having low affinity to opsonins, thus enhancing circulation time of the devices in blood before they reach the targeted sites[100]. Thirdly, they should be biodegradable, non-toxic, biocompatible and non-immunogenic[101].

1.5. CNS targeting mechanism

One essential part of the nanocarrier system is the conjugation of the appropriate BBB-targeting mechanism. Other than those with a polysorbate-80 coating or a small molecular size, most drug-carrying nanoparticles require the use of one of the native BBB transport routes for macromolecules, as illustrated in Fig. 2. Water soluble agents dissolve through tight junctions via the paracellular aqueous pathway while lipid-soluble agents dissolve trans-cellularly through the lipid plasma membrane. However, for almost all other substances, the other three pathways, namely the carrier (CMT), receptor-mediated (RMT), and absorptive- mediated (AMT) systems are required. CMT relies on the conformational change of membrane transport proteins to move solutes such as glucose and amino acids along with their concentration gradient. RMT, on the other hand, is triggered by a ligand-receptor interaction which induces endocytosis of the molecule into the brain, while AMT on electrostatic interaction. Via these pathways, the BBB shuttles metabolic compounds like insulin or low-density lipoprotein (LDL) across the membrane and once modified, nanoparticles can take advantage of these systems to non-

invasively deliver neuroactive drugs to the CNS[90]. As PEG is highly recommended for surface grafting in order to provide steric stabilization and decrease the rate of elimination from the blood into the liver or spleen, ligands can be attached to the nanocarrier via the PEG chain so that they extend past the PEG corona for more effective targeting[102].

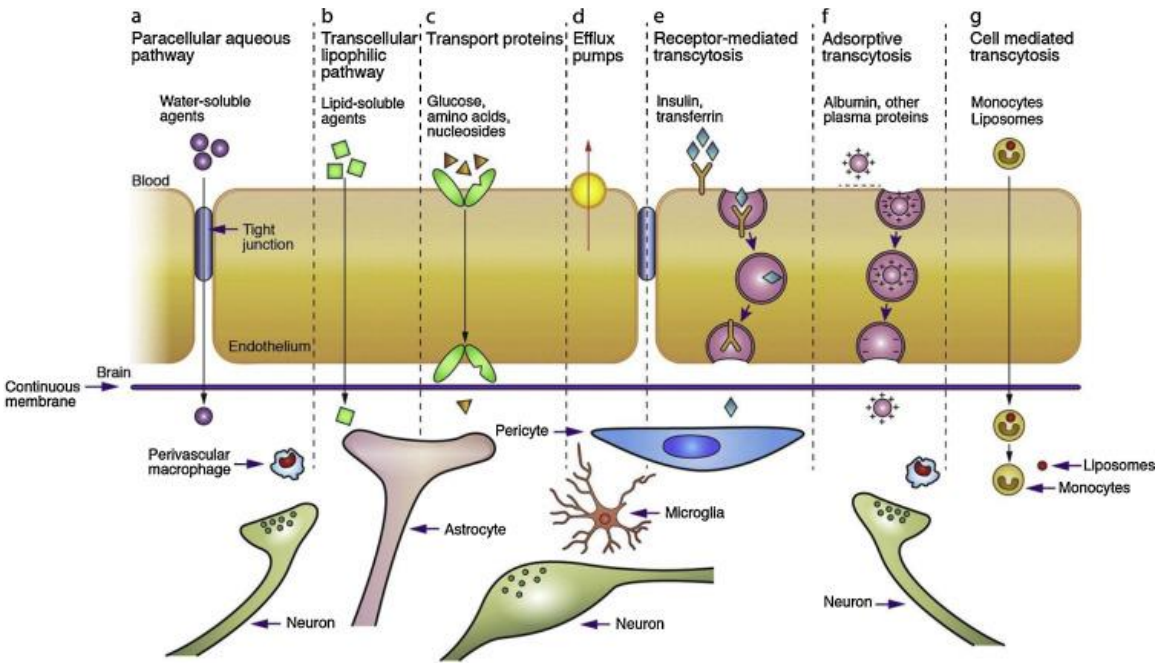

Figure 1.5 Different BBB penetrate pathways

1.5.1. Carrier-mediated transport (CMT)

Nutrients such as glucose, lactose and neutral amino acids required for survival are brought into the brain using membrane proteins expressed at the surface of the BBB. One of such highly expressed proteins is the glucose transporter (GLUT1) that promotes the intake of D-glucose and glucose analogs from the blood into the brain[14]. Drugs themselves can be chemically altered to resemble these nutrients as in the case of L-DOPA, or the substrates of the transporters could be conjugated to drug-loaded nanocarriers[103]. The applications of these methods are limited, however, as the drug/ligand must be very small and similar in structure to the nutrient. Furthermore, as the carrier protein is located at the membrane, the drug must still be moved via diffusion across the cell membranes at the BBB to penetrate into the brain itself[90].

1.5.2. Receptor-mediated transport (RMT)

Unlike CMT, the RMT mechanism exists for the intake of larger molecules such as insulin or transferrin[104]. The contact of either the natural ligand or an artificial form (antibody) with the membrane receptor induces endocytosis of the macromolecule into an intracellular transport vesicle, which can then cross the endothelium lining of the BBB to be released into the brain[104]. The transferrin receptor (TfR) has been the most widely characterized RMT system for drug delivery, as it has proven to be an efficient cellular uptake pathway for anticancer drugs, while also being over-expressed in many tumors[105]. Thus, much research has been focused on either attaching transferrin or an antibody against transferrin to one of the above nanocarriers to facilitate the transport of large drug molecules[102].

Transferrin-coated PLGA nanoparticles caused a 20-fold increase in the targeting of an in-vitro BBB model as compared to non-coated particles, as reported by Chang et al. (2009)[105]. It was confirmed via fluorescence microscopy that the particles entered by means of endocytosis. Similarly, lactoferrin, a protein of the transferrin family, also induced uptake in an in-vitro and in-vivo model, when attached to PEG-PLA nanoparticles[106]. A significant disadvantage of conjugating such proteins to the surface of particles is the following competition with endogenous transferrin for binding of the receptor, thus either inhibiting the brain's natural uptake of transferrin or discrediting the effectiveness of the particle[107].

Currently, RMT has shown much promise for the successful delivery of anticancer compounds to brain tumors. Multiple studies have reported an upregulation in expression of the transferrin receptor on metastatic and drug-resistant tumors, and a diphtheria toxin mutant covalently bound to transferrin (Tf-CRM107) is now being tested in human clinical trials for the treatment of glioblastoma[108].

1.5.3. Absorptive-mediated transport (AMT)

The last of the transport routes explored for BBB drug delivery is the AMT system, which relies on the electrostatic interaction between a positively charged moiety and the negatively charged endothelial cell membrane[14]. Initially, its application was isolated to cationized albumin nanoparticles as it was demonstrated by researchers such as Pardridge et al. that these particles were capable of delivering drugs and peptides to the cerebral parenchyma[109].

Later, the concept of cell-penetrating peptides (CPPs) developed as positively charged peptides of length less than 30 amino acids that were able to penetrate cell membranes via AMT[102]. One of the more prominent examples is the HIV-1 trans-activating transcriptor (TAT) peptide. When TAT-derived CPPs bind to the surface of the cell, they induce macropinocytosis, allowing unusually large molecules, including full-length fusion proteins[110], to make their way across the BBB.

However, as AMT only relies on electrostatic attraction, the lack of tissue specificity poses a challenge for both limiting drug concentration in non-target organs and achieving the desired therapeutic drug level in the brain. These issues have to be assessed before AMT can be implemented clinically[111].

1.6. Motivation and research goals

The primary motivation behind this work was to increase the brain delivery of antiretroviral therapies using suitable nano-carrier systems in order to ease the mobility and mortality of HAND. The goal of the study was to develop a transferrin conjugated nanoemulsion system to increase the brain concentration of antiretroviral medications. The specific research goals are listed below:

1. Formulation of the brain targeted nanoemulsion system (Chapter 2).
2. Formulation optimization and physicochemical characterization of darunavir loaded transferrin conjugated nanoemulsion system (Tf-NE-DRV) (Chapter 3).
3. In vitro activity of Tf-NE-DRV (Chapter 4).

4. In vivo biodistribution of Tf-NE-DRV and future directions (Chapter 5).

1.7. Thesis organization

This thesis consists of five chapters. The first chapter is the general introduction of major nano delivery systems, the method of preparation, a brief review of HAND and the challenge of highly active antiretroviral therapy. The second chapter focuses on the formulation of the brain targeted the nanoemulsion system. The third chapter deals with the formulation optimization and physicochemical characterization of darunavir loaded transferrin conjugated nanoemulsion system (Tf-NE-DRV). In vitro activity of Tf-NE-DRV was explored in Chapter Four. Chapter five deals with In vivo biodistribution of Tf-NE-DRV and future directions.

CHAPTER 2

FORMULATION OF THE CNS TARGETED NANOEMULSION SYSTEM

2.1. Abstract

After reviewing the features of the different nanoparticle system, we decided to utilize the nanoemulsion system for drug delivery. An oil-in-water (O/W) nanoemulsion system consists of an oil core surrounded by a single layer of amphiphilic surfactants. Since we are trying to achieve brain delivery, we try to use safe and biocompatible materials. For the surfactants in the system, we decided to use phospholipids DSPC and DSPE-PEG (2000). We did some testing using two different stabilizers, cholesterol and tripalmitin, and two different oils, which are docosahexaenoic acid (DHA) and Capmul MCM C8. All four groups of formulation gave a good size distribution. But compared to tripalmitin and Capmul MCM C8, cholesterol and DHA are endogenous and can help to avoid unnecessary safety issue from the material perspective. That's why we decided to proceed using cholesterol as stabilizer and DHA as oil core. Transferrin receptor has been widely studied as a beneficial medium to bypass the Blood-Brain Barrier (BBB). We plan to achieve CNS delivery through coupling transferrin externally on the nanoemulsion system. NHS ester crosslinking method was utilized, and the coupling efficiency test was performed with for different lipid to transferrin ratios (w/w). Decent amount of coupling was achieved for all the sample groups.

2.2. Introduction

Oil-in-water (O/W) nanoemulsion is kinetically stable heterogeneous colloidal systems consisting of droplets of oil dispersed in the immiscible continuous phase surrounded and stabilized by the amphiphilic surfactant film.[112] Nanoemulsions are typically prepared in a two-step process where a macroemulsion is first prepared and is then converted to a nanoemulsion in the second step.[113]

2.2.1. 1,2-distearoyl-sn-glycero-3-phosphocholine (DSPC) and 1,2-Distearoyl-sn-glycero-3-phosphoethanolamine (DSPE)

Phosphatidylethanolamine (PE) and phosphatidylcholine (PC) are two different classes of phospholipids found in biological membranes[114]. We chose to use these two types of phospholipids as the main structure of our nanoemulsion systems. These amphiphilic lipids can serve as a surfactant in the whole systems. Since we are trying to achieve CNS delivery, we don't want to bring too many exogenous materials into the brain, which would cause additional problems.

As hydrophobic nano-systems are cleared quickly, it seems logical to assume that making their surface hydrophilic would increase their time in circulation. In fact, coating the nano-system with polymers like polyethylene glycol (PEG) has been proven valuable[115, 116]. PEG is a hydrophilic and relatively inert polymer that when incorporated in the nanoparticle surface, hinders the binding of plasma proteins (opsonization). PEGylated nanoparticles are often referred to as "stealth" nanoparticles because, without opsonization, they remain undetected by the reticuloendothelial system (RES)[117]. To achieve longer circulation time of our nanoemulsion system, we used PEGylated DSPE

as the main structure, which will further increase the medication accumulation at the disease site.

2.2.2. Transferrin receptors serving as a promising target for brain delivery

Diseases related to the brain have long been a challenging area for both clinical practitioners and medical researchers. The main obstacle in brain-related diseases is the presence of blood-brain barrier (BBB), which selectively regulates and limits the amount and types of therapeutic agents permeating into the brain parenchyma[118]. Non-invasive approaches are imminent to be discovered and developed in view of the advantages of manipulating endogenous transport systems to overcome the BBB without physically interfering with the brain tissues which otherwise may cause medical complications[119]. Among the receptors found to date, transferrin receptors have been widely studied and shown to be a promising molecular probe for targeted drug delivery to the brain. The mechanism of how transferrin works are showed in Figure 2.1. Since BBB prevents free diffusion of iron into the brain tissue, the brain needs a specialized system that facilitates such uptake. Iron is indispensable for the brain tissue, because it serves as an important co-factor in many metabolic processes like ATP synthesis as part of the iron-sulfur cluster and heme in the mitochondrial respiratory chain complexes. Transferrin receptors are present on endothelial cells of the brain, but not on endothelial cells elsewhere in the body, which makes them very interesting targets for vascular drug delivery[120].

Transferrin-conjugated nanoparticles have the potential to achieve the therapeutic dose of anti-HIV drugs to the brain, this could be effective in controlling the viral replication in

the CNS and eventually preventing neurological complications associated with HIV infection. A well-developed CNS drug delivery system could potentially be used in the treatment of other neurological conditions such as Alzheimer or Parkinson's disease.

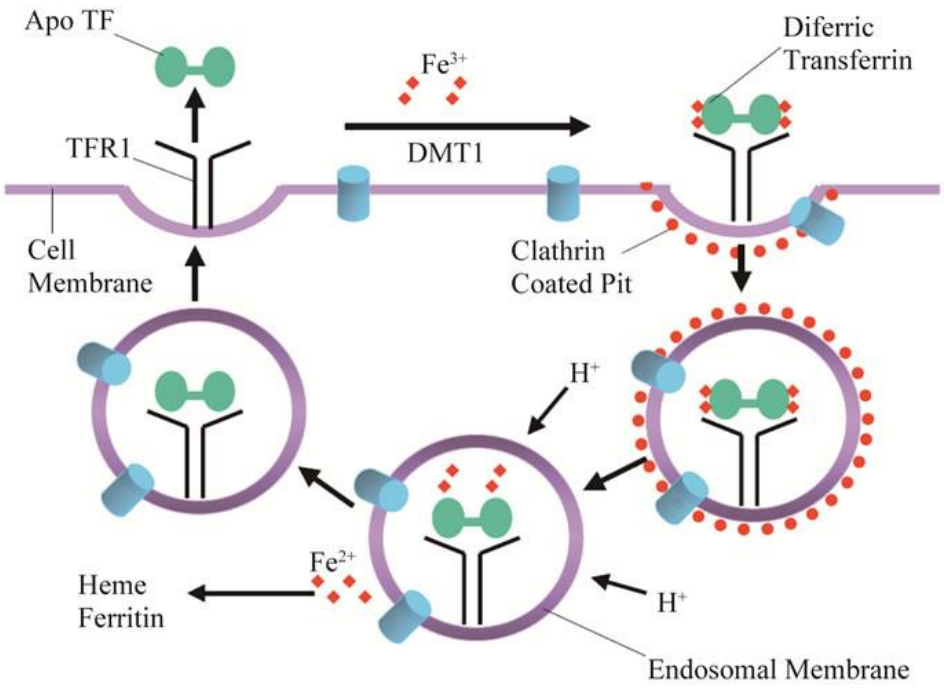

Figure 2.1 Transferrin function mechanism

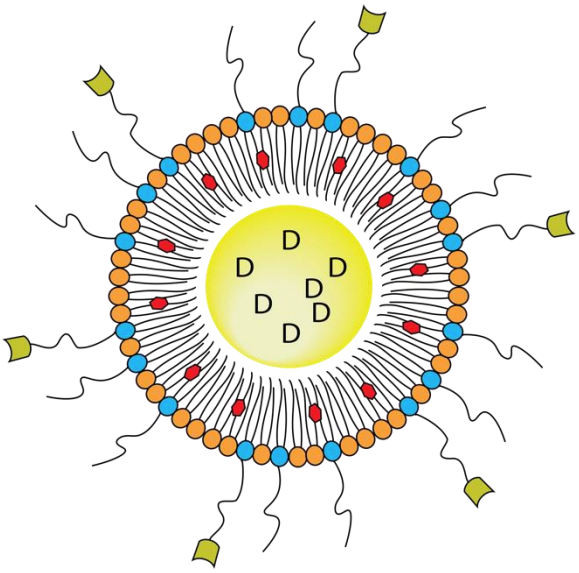

Figure 2.2. Illustration of our novel nanoemulsion

2.3. Experimental Section

2.3.1. Materials

1,2-distearoyl-sn-glycero-3-phosphocholine (18:0 PC, 850365), 1,2-distearoyl-sn-glycero-3-phosphoethanolamine-N-[methoxy(polyethylene glycol)-2000] (ammonium salt) (18:0 PEG2000 PE, 880120), 1,2-distearoyl-sn-glycero-3-phosphoethanolamine-N-[maleimide(polyethylene glycol)-2000] (ammonium salt) (DSPE-PEG(2000) Maleimide, Avanti, 880126), Cholesterol, 1,2-dioleoyl-sn-glycero-3-phosphoethanolamine-N-(lissamine rhodamine B sulfonyl) (ammonium salt) (18:1 Liss Rhod PE, 810150) were all purchased from Avanti Polar Lipids, Inc. Holo-Transferrin human (Tf), S-

Acetylthioglycolic acid N-hydroxysuccinimide ester (SATA) and Hydroxylamine hydrochloride were purchased from Sigma-Aldrich.

2.3.2. Preparation of Transferrin conjugated DSPE-PEG (2000)-Maleimide

To prepare for maleimide-micelles, 4.0mol DSPE-PEG (2000) Maleimide (25mg/ml) was used, and solvent chloroform was evaporated using nitrogen gas and vacuum dryer. Suspend film of lipid was then dissolved in a pre-warmed solution (65 degrees, 20mM HEPES, 135mM NaCl, pH 7.3).

To prepare transferrin for conjugation, 10 ul (1.25nM) transferrin solution was mixed with a 40uL buffer consisting of 20mM HEPES, 150mM NaCl and 10mM EDTA at pH7.5. 10nM SATA solution was then mixed with transferrin in a molar ratio of 8:1 and let them react for 45 minutes at room temperature to make the Tf-SATA solution. 51uL of the Tf-SATA solution was then mixed with 5.1uL Hydroxylamine HCl to react for 2 hours at room temperature. The chemical reaction mechanism was presented in Figure 2.3 and Figure 2.4. After sufficient reaction, the mixture was then purified on a spin desalting column (Pre-equilibrium with HEPES, NaCl pH 7.5, 0.1mM EDTA) to remove excess SATA and hydroxylamine. Conjugation was then performed by adding the transferrin-SH solution (elute from desalting column) to maleimide-micelles and letting them react overnight at room temperature. Samples were lyophilized and stored at -20C for future usage. (Figure 2.5)

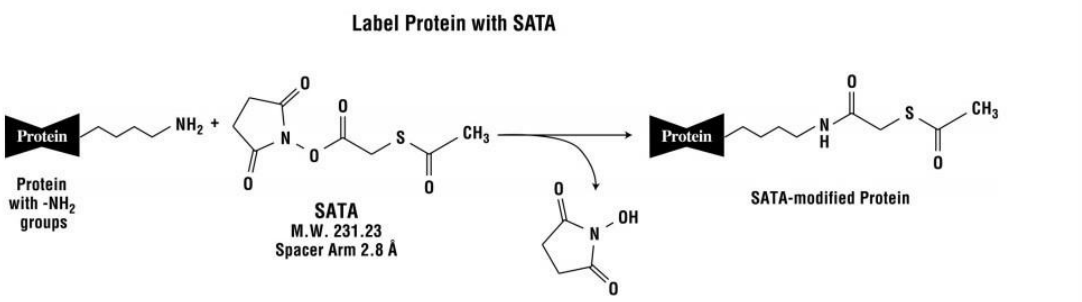

Figure 2.3 The reaction of SATA with a primary amine

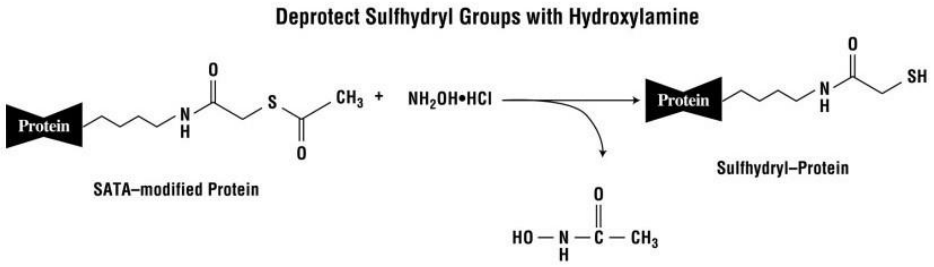

Figure 2.4 The deprotection with hydroxylamine to generate a sulfhydryl

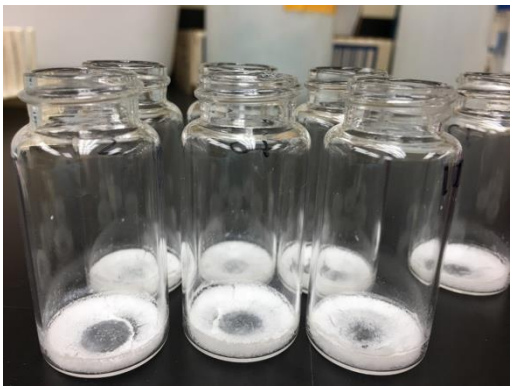

Figure 2.5 Lyophilized transferrin conjugated micelles

2.3.3. Quantification of Transferrin conjugation efficiency

Fluorescent label, fluorescein isothiocyanate (FITC) was used to make transferrin quantifiable through Fluorescent signal using plate reader. Transferrin-conjugated DSPE-PEG (2000)-Maleimide can be inserted into the nanoemulsion while free transferrin stays in the solution. Free transferrin was separated from nanoemulsions using centrifuge tubes (Vivaspin® 500 Centrifugal Concentrator). Conjugation efficiency was calculated by measuring the fluorescence signal of FITC labeled transferrin.

2.3.4. Formulation of Transferrin conjugated nanoemulsion

Solvent evaporation and the sonication method were used to make transferrin conjugated nanoemulsion (Figure 2.6). The ratio of different lipid components was not optimized in this project, and I just followed the recipe from previous research in our lab. Cholesterol, DSPC, DSPE-PEG (2000) are mixed in a weight ratio of 0.5:4:3. Oil was added by a different percentage according to the different formulation recipe. The mixture is then dried using nitrogen gas to get rid of most of the chloroform completely. 110uL dichloromethane (DCM) and 1mL biotech water are then added and vortexed for the 30s. Then, sonication is performed with lid closed for 1 min followed by continuous sonication with the lid open until the solution becomes transparent and continue for 30s more. Usually this process last 5min. The prepared sample was then stirred slowly for two hours at room temperature to evaporate all the potential DCM residuals.

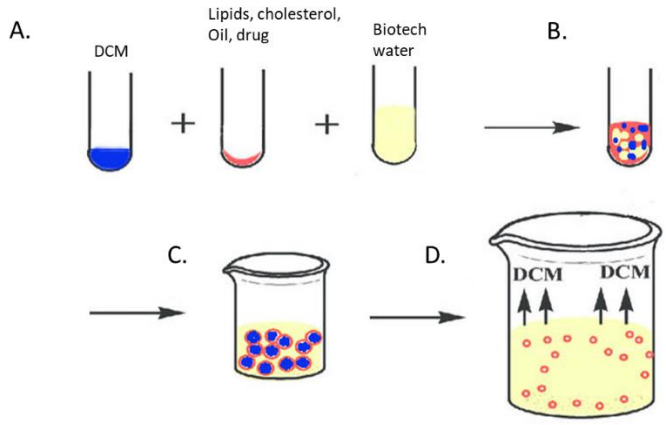

Figure 2.6 Illustration of nanoemulsion preparation. A. DCM and Biotech water to dried lipids, cholesterol, oil and drug mixture. B. vortex to thoroughly mix all the components. C. Coarse macroemulsion is formed after vortex and close lid sonication. D. nanoemulsion is formed through continuous sonication.

2.3.5. Size Distribution and zeta potentials

Particle size and zeta potential values were measured by photon correlation spectroscopy using Malvern Zetasizer NanoZS90 (Worcestershire, UK). For the size and zeta measurement around 15-30 μL of fresh sample was suspended in 1 mL of distilled de-ionized water and 15 successive cycles were run at 25 °C. A lot of research groups prefer to filter the sample before size analysis, but for this study, all the size measurements were done without filtration. Size data based on the distribution by intensity were presented.

2.4. Results and Discussion

2.4.1. Stabilizers and oils

Cholesterol has been widely used in nanoparticle systems as a stabilizer, which can embed between phospholipid structures. Through the interaction with the phospholipid fatty-acid chains, cholesterol increase membrane packing, which both maintains membrane integrity and modulates membrane fluidity.[121] Tripalmitin has been successfully used as a stabilizer based on previous research from our lab. So, we did a test using these two different stabilizers with two different kinds of oil, which is docosahexaenoic acid (DHA) and Capmul MCM C8. In regard to the choice of oil, we will discuss more in Chapter 3.

Nanoemulsions were prepared using different stabilizer and oil, and the size and polydispersity index (PDI) is summarized in table 2.1. PDIs were all smaller than 0.3 which indicates a narrow size distribution. Considering 100nm is the optimum size for a

nanoparticle-based on the literature evaluation and discussions so far. At this size, the particle could pass BBB and diffuse freely in the brain parenchyma, sufficient amount of drug delivery due to the high surface area to volume ration, and avoiding immediate clearance by the lymphatic system.[122] Sizes within the range between 80nm to 100nm are all acceptable.

Cholesterol is essential for all animal life; each cell is capable of synthesizing it. Furthermore, it can be absorbed directly from animal-based foods.[121, 123] DHA is the most abundant omega-3 fatty acid that is a primary structural component of the human brain, cerebral cortex, skin, and retina.[124] Since we try to avoid exogenous materials in our nanoemulsion systems, cholesterol was chosen as a stabilizer while DHA was chosen as the oil core.

For our nanoemulsion system, we tend to make it neutral on surface charge, so it can better interact with BBB to achieve brain delivery. In this case, we won't measure the zeta potential any more in the following research, since the Zeta potential of the nanoemulsion is designed to be close to zero.

Table 2.1

Size and PDI summary table of nanoemulsion formulation with different stabilizers and oils

Phospholipids	**Stabilizer**	**Oil**	**Size (nm)**	**PDI**
DSPC and DSPE-PEG (2000)	Cholesterol	DHA	93.02±4.33	0.197±0.0026
DSPC and DSPE-PEG (2000)	Cholesterol	Capmul MCM C8	84.62±6.64	0.241±0.0262
DSPC and DSPE-PEG (2000)	Tripalmitine	DHA	85.51±6.38	0.242±0.0160
DSPC and DSPE-PEG (2000)	Tripalmitine	Capmul MCM C8	67.11±2.31	0.291±0.0131

2.4.2. Transferrin conjugation efficiency

Different amount of transferrin was added to the same amount of lipids for reaction. Four different amounts were tested, and they were about 20ng, 40ng, 60ng, and 80ng. In this thesis, they were expressed in the form of total lipid weight to transferrin weight ratio as 40:1, 20:1, 12:1 and 10:1. As shown in Fig.9, the conjugation efficiencies are similar to each other within different samples, which is between 80% to 90%. This is relatively high conjugation since the NHS ester crosslinking reaction is a high-efficiency reaction.

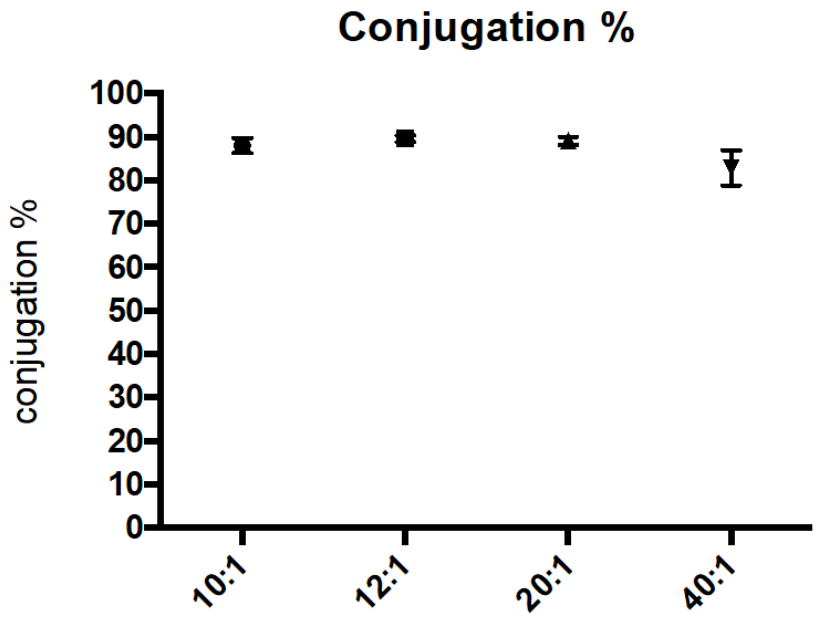

Figure 2.7 Conjugation efficiency for the different weight ratio of total lipids to transferrin protein, 10:1, 12:1, 20:1 and 40:1.

2.5. Conclusion

As a stabilizer, cholesterol and tripalmitin both work fine. To some extent, tripalmitin is slightly better than cholesterol by comparing the size. Smaller size represents that lipids are better aligned and packed with the existence of tripalmitin. The nanoparticles are more rigid and compact in this case. But rigidity is not always a useful feature for nanoparticles, and you have to take different applications into consideration. [125] However, we decided to use cholesterol and DHA since they are endogenous to the brain. Transferrin coupling is very efficient using the NHS ester crosslinking method. A significant difference was not observed between the range 10:1 to 40:1 (lipids to transferrin ratio w/w).

CHAPTER 3

FORMULATION OPTIMIZATION AND PHYSICOCHEMICAL CHARACTERIZATION OF DARUNAVIR LOADED TRANSFERRIN CONJUGATED NANOEMULSION (TF-NE-DRV)

3.1. Abstract

In this chapter, a brain targeted nanoemulsion system known as darunavir loaded transferrin conjugated nanoemulsion (Tf-NE-DRV), in which highly lipophilic drug darunavir was dispersed in the oil phase, DHA. Tf-NE-DRV was formulated by an emulsification solvent evaporation technique. The particle size was measured by dynamic light scattering and TEM was also performed to further investigate the morphology of Tf-NE-DRV. The nanoparticles were evaluated for thermal properties by differential scanning calorimetry (DSC). Drug loading, encapsulation efficiency and in vitro drug release at 37°C were spectrophotometrically measured. Stability of Tf-NE-DRV samples in different mediums was also evaluated. Differential scanning calorimetry analysis revealed that darunavir was uniformly dispersed in the system, which subsequently led to improved drug release kinetics with sustained release.

3.2. Introduction

As we discussed in chapter 1, anti-retroviral therapies, especially protease inhibitors, has the most limited access to CNS. All most of the compounds in this category can't reach a therapeutic concentration in CNS due to the active efflux transporter expression on the membrane of cells that constitute the BBB.[126] However, darunavir is one of them. The computed and experimental properties of Darunavir is summarized in table 3.1. The

limited water solubility and the logP value make it an ideal candidate for our nanoemulsion system. Darunavir, under the brand name Prezista, was approved by the FDA quite recently in 2006. The emergence and transmission of antiretroviral drug resistance have been and remain a concern among people living with human immunodeficiency virus (HIV)-1 infection. During the more than 10 years' approval, Darunavir demonstrated a high barrier to resistance.[126] Under these circumstances, we don't need to worry too much about resistance development since we are developing this single antiretroviral therapy formulation.

Darunavir is primarily metabolized by cytochrome P450 3A4 (CYP3A4). Common side effects include diarrhea, nausea, abdominal pain, headache, and rash. Severe side effects include allergic reactions, liver problems, and skin rashes such as toxic epidermal necrolysis. Darunavir is often used with ritonavir or cobicistat, which inhibit CYP3A, thereby increasing the bioavailability and half-life of darunavir.

Darunavir is approximately 90% bound to plasma proteins while CNS protein binding is less than 10%. Based on the clinical data, darunavir concentration in the CSF sample is only around 0.9% of plasma concentration.[127] The result of the clinical research suggested that active efflux transporter must be involved in the darunavir brain penetration process.

Table 3.1 Computed and experimental properties of Darunavir

Property Name	**Property value**
Molecular Weight	547.667g/mol
Hydrogen Bond Donor Count	3
Hydrogen Bond Acceptor Count	9
Rotatable Bond Count	12
Complexity	853
Topological Polar Surface Area	149 A^2
Color	White, amorphous solid
Melting Point	74 C
Water Solubility	Approximately 0.15mg/ml at 20℃
LogP	1.8

Although the intestinal absorption of darunavir has been intermediate-to-high when using Caco-2 monolayers, darunavir classification according to the BCS is not defined. Its permeability is not defined, and there are no published studies on its solubility according to the BCS criteria. However, some inferences can be made about the biopharmaceutical classification of darunavir. [128] [129] Taking pharmacology and PK data into account, it is possible to say that darunavir, when administered with ritonavir, can behave like a highly permeable drug substance and its biopharmaceutical classification may be in class I or II depending on its solubility. Darunavir is a drug of relatively low aqueous solubility and, therefore, it is likely to be classified as class II.[130]

3.3. Experimental section

3.3.1. Materials

1,2-distearoyl-sn-glycero-3-phosphocholine (18:0 PC, 850365), 1,2-distearoyl-sn-glycero-3-phosphoethanolamine-N-[methoxy(polyethylene glycol)-2000] (ammonium salt) (18:0 PEG2000 PE, 880120), 1,2-distearoyl-sn-glycero-3-phosphoethanolamine-N-[maleimide(polyethylene glycol)-2000] (ammonium salt) (DSPE-PEG(2000) Maleimide, Avanti, 880126), Cholesterol, 1,2-dioleoyl-sn-glycero-3-phosphoethanolamine-N-(lissamine rhodamine B sulfonyl) (ammonium salt) (18:1 Liss Rhod PE, 810150) were all purchased from Avanti Polar Lipids, Inc. Darunavir (SML0937) was purchased from Sigma-Aldrich.

3.3.2. Solubility test of darunavir in different oils

Darunavir can freely dissolve in a few different oils and surfactants. They are Tween 80, Capmul MCM, Capmul PG8, Captex 200 and Capmul MCM C8. 1ml of each oil or surfactant was measured and put in a transparent glass vial, 1mg darunavir was measured and added to each vial. All five samples were stirred at the same speed at room temp. samples were visually checked every minute.

3.3.3. Fabrication of darunavir loaded Tf conjugated nanoemulsion system （Tf-NE-DRV）

The solvent evaporation/sonication method was used to make Tf-NE-DRV. Cholesterol, DSPC, DSPE-PEG (2000) were mixed in a weight ratio of 0.5:4:3. Different amount of DHA, darunavir and Tf conjugated micelles were added accordingly. The mixture was then dried using nitrogen gas to get rid of the chloroform completely. 110uL dichloromethane (DCM) and 1mL biotech water were then added and vortexed for 30 seconds. Then, sonication was performed with lid closed for 1 min followed by continuous sonication with the lid open until the solution became transparent and continued for 30s more. Usually, this process lasts for 5min. The prepared sample was then stirred slowly for two hours at room temperature to evaporate all the potential DCM residuals.

3.3.4. Encapsulation efficiency (EE)

Each nanoparticle sample freshly prepared was centrifuged at 15,000 rpm at 16 ºC for 10 min using 30kD microcentrifuge tube. The unencapsulated drug was separated into the

supernatant. The nanoemulsions part was dissolved in methanol, and the amount of drug entrapped was spectrophotometrically analyzed using Spectramax M2 microplate reader (Molecular Devices, Sunnyvale, CA) by UV signal at 266 nm for darunavir. The linear calibration curve for darunavir was obtained in methanol in the range of 100 μg/ml to 0 μg/ml. Blank, drug-free nanoparticles served as the background control, and we did not detect significant absorbance at the selected wavelengths. Experiments were repeated in triplicate.

EE values were calculated according to the following formula:

EE (%) = (Amount of drug encapsulated / Amount of drug added) * 100%

3.3.5. Size distribution and zeta potentials

Particle size values were measured by photon correlation spectroscopy using Malvern Zetasizer NanoZS90 (Worcestershire, UK). Tf-NE-DRV fresh samples were suspended in distilled water, and 15 successive cycles were run at 25 °C. Size data based on the distribution by intensity were presented.

3.3.6. Transmission electron microscopy (TEM)

The morphology of nanoparticles was determined by transmission electron microscope using JEOL, JEM-1400 TEM (Tokyo, Japan) at 120 kV. A drop of nanoemulsion suspension (concentration: 0.5 mg/ml) was placed on a 400-mesh copper grid (Ultra-thin

carbon type A, Ted Pella Inc., Redding, CA). Samples were air-dried in the hood before the examination.

3.3.7. Differential scanning calorimetry (DSC)

DSC analysis was carried out to evaluate the drug dispersion in the nanoemulsion system. Samples each containing 1-2 mg lyophilized Tf-NE-DRV were weighted in aluminum pans, sealed, and equilibrated at 20 °C for 10 min. Trehalose was added before lyophilization as the cryoprotectant. The analysis was performed using a DSC Q200 differential scanning calorimeter (TA Instruments, New Castle, DE) at a heating rate of 2 °C/min from 2 to 100 °C. Data were collected and analyzed using software TA Universal Analysis 2000.

3.3.8. Stability of Tf-NE-DRV in PBS and cell culture medium

Each nanoemulsion sample was resuspended in PBS buffer (or cell culture medium) to make 10% final concentration. Samples were stored at 37℃. At preselected time intervals, 15 – 30ul samples of nanoemulsions were diluted in 1ml distilled deionized water and characterized for size.

3.3.9. In vitro drug release of Tf-NE-DRV

The amount of drug released in the PBS buffer was determined directly by measuring the drug content in the buffer system. For the drug release study, the nanoemulsions were separated as described in the earlier section. Each nanoemulsion sample was transferred to Tube-O-Dialyzer (Medi, MWCO = 1 kDa) and the tube was placed in 25ml

of release medium (PBS at pH 7.4 with 2% tween 80) at 37 ºC under magnetic stirring. The volume of medium used has exceeded the manufacturer's recommended standard for maintaining the sink conditions. At each selected time point, release medium samples were withdrawn, and the released drug content was determined using the HPLC method at 1ml/min flow rate. Experiments were repeated in duplicate. The linear calibration curve for darunavir was obtained in methanol in the range of 1000 μg/ml to 1 μg/ml. The running buffer is 60% acetonitrile in Distilled deionized water. Blank, drug-free nanoparticles served as the background control, and we did not detect a significant peak at the residual time (RT) of darunavir.

3.4. Results and discussion

3.4.1. Solubility test of darunavir

1mg of darunavir compounds were added to each oil and surfactants sample. Samples were visually checked every minute. Capmul MCM C8 completely dissolved the compound first. Although the solubility in Capmul MCM C8 may not be the biggest, the rate of dissolving is critical during the preparation of the nanoemulsion.

3.4.2. Morphology and size evaluation

As I mentioned in chapter 2, the ratio of phospholipids and cholesterol were set by simply following previous research. Different percentage of oil was added to the formulation, 5%, 10%, 15% and 20% (oil to lipids ratio, w/w). The size, PDI of formulated particles were measured at 5%, 10%, 15% and 20% drug loading (drug to lipids ratio, w/w). The data is presented in Fig 3.1. The sizes were in the range of 80nm to 150nm. When the oil

amount was smaller than 15%, the particle sizes were all around 100nm no matter how many drugs were loaded. But once the oil amount reached 20%, the size significantly increased. Oil amount seemed to be the dominant factor in the size. The energy to prepare the formulation was set in our method and it won't be strong enough to break macroemulsions into fine enough nanoemulsions once the oil amount exceeds a certain limit. It could also due to the smaller surfactant to oil ratio causing the increase of size. The oil is the medium to carrier drug in the whole system. As you can see from the PDI data, the more oil in the system, the smaller the PDI we can get.

From 13 groups of formulation above, we chose 4 best ones to add transferrin on using the following two criteria, small PDI and best size. Size and PDI were summarized in Fig.3.2. 4 different amounts of transferrin were added to each formulation. From the size charts, we can see that in general, the size didn't change significantly after adding the transferrin to the surface, while the PDIs were increased around 0.1 unit. Transferrin is only 86kD; it's not big enough to cause size increase. On the contrary, the complexity of the system was increased. That's the reason why PDI was increased.

Transmission electron microscopy (TEM) was used to understand the morphology better. Please refer to Fig 3.3A and 3.3B. Nanoemulsion droplets appeared as dark vesicles in the images. The particles were spherical in shape, and the average size was found to be around 100nm, which accorded with DLS data. The highly magnified TEM image clearly shows the compact spherical structure of Tf-NE-DRV.

A.

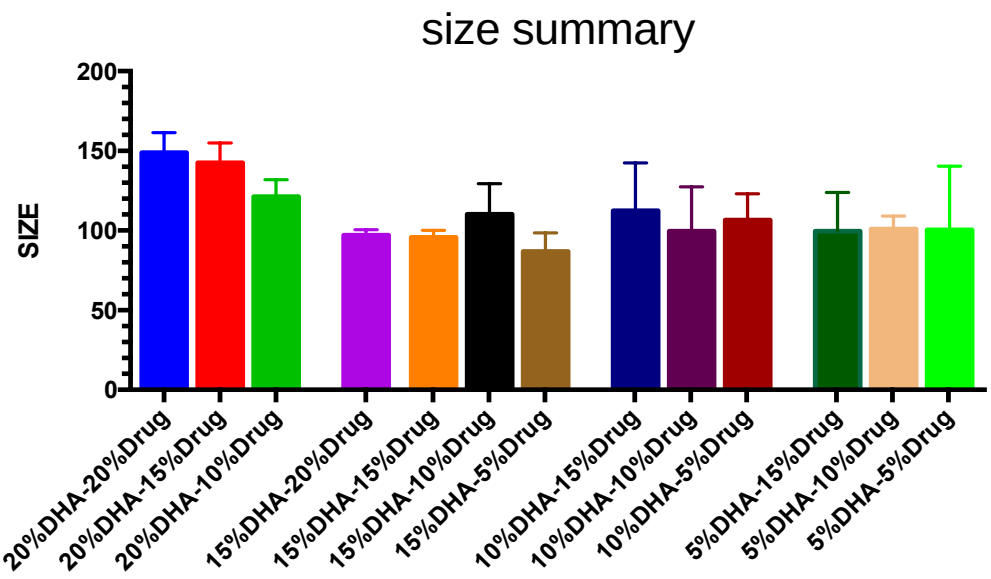

B.

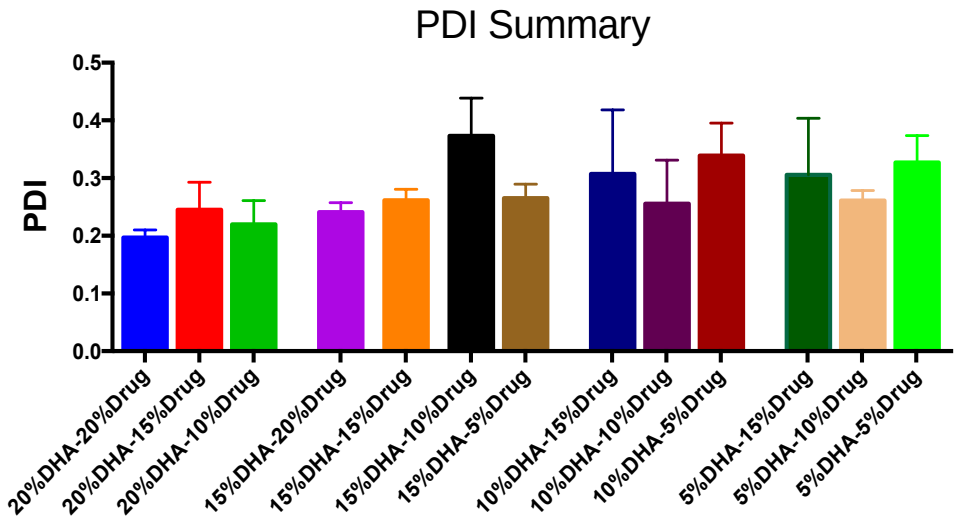

Figure 3.1 (A) Size summary of all the formulations. (B) PDI of all the formulations.

All the percentage is w/w of total lipids

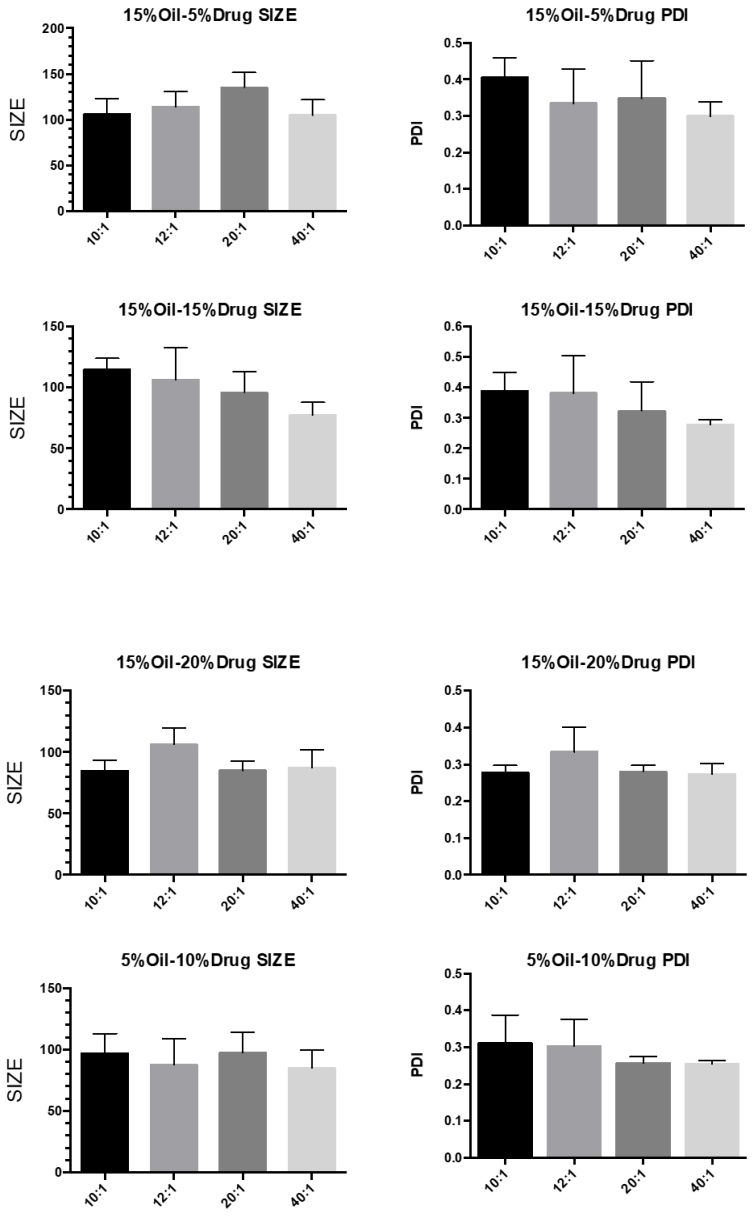

Figure 3.2 Selectively add a different amount of transferrin to four different formulations. They are 15% oil-5% drug, 15% oil-15% drug, 15% oil-20% drug and 5% oil-10% drug. Size and PDI with different amount of transferrin were summarized above.

A.

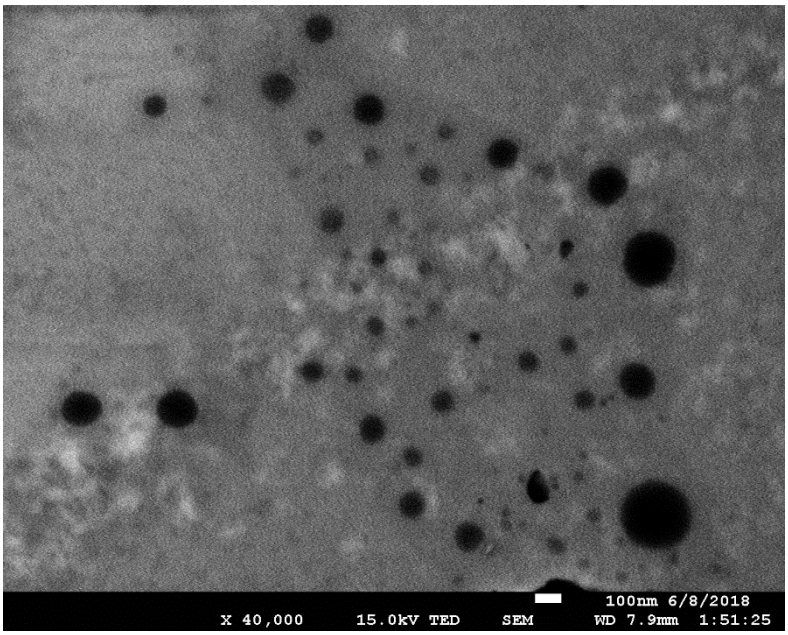

B.

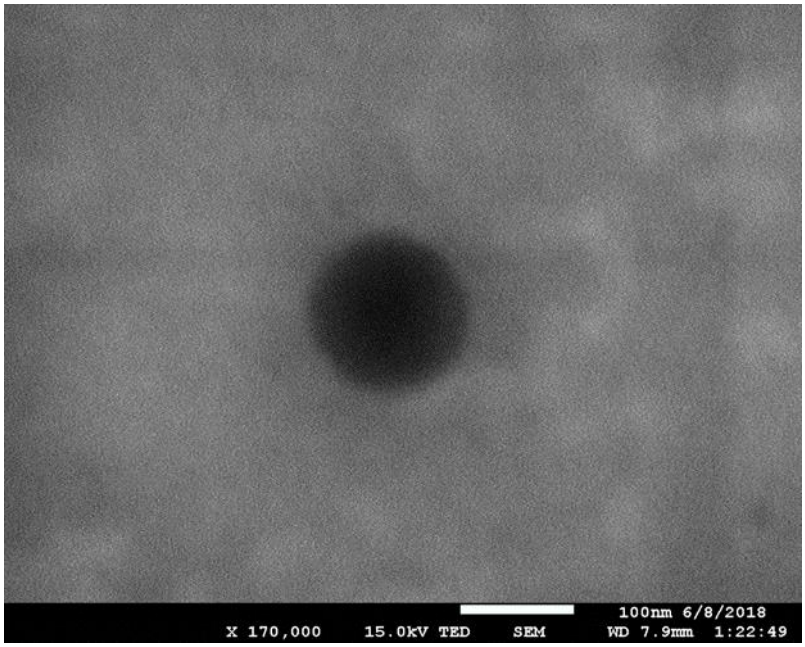

Figure 3.3 (A) Transmission electron microscope (TEM) images of Tf-NE-DRV (10:1-15% oil – 20% drug) under low magnification (X40,000) and (B) high magnification (X 170,000).

3.4.3. EE and stability of Tf-NE-DRV

We only kept two formulations with best size and PDI for the following studies. Drug encapsulation efficiency (EE) results for these two formulations were presented in Figure 3.4. The EE was not affected by the external Tf amount. 20% oil-15% drug Tf-NE-DRV had around 10% more efficiency than 5% oil -10% drug Tf-NE-DRV in average due to the larger oil to drug ratio. Actual drug amount encapsulated was calculated based on the following equation:

Amount of drug encapsulated = Drug loading X EE X 100%

So, 20% oil-15% drug Tf-NE-DRV had more drug encapsulated, which is around 12% of the total lipids weight.

Stability study was performed in PBS and cell culture medium at 37℃ for 5 consecutive days. The primary intent behind this study was to make sure these two formulations are stable in future assay conditions, and the stability won't affect the results. From Figure 3.5, all the particle sizes were around 100nm and didn't change during the period of time. PDIs also maintained the trends. All the formulations tested were stable in PBS at 37℃ for 5 days. Figure 3.6 is the size and PDI of samples in the cell culture medium. Due to a large number of proteins inside the medium, the size and PDI didn't reflect the real value. But from the trend of size, we can tell most of the groups were stable.

A

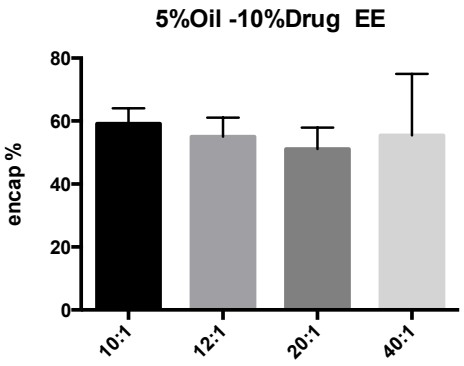

B.

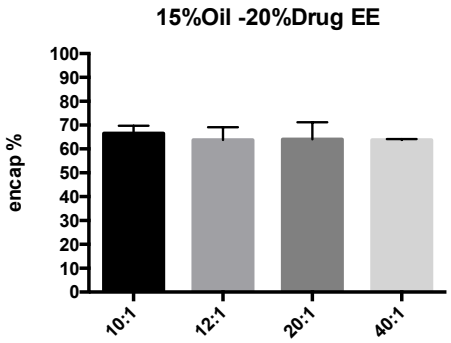

Figure 3.4 (A) Drug encapsulation efficiency of 5% oil-10% drug formulation with different amount of transferrin on the surface. (B) Drug encapsulation efficiency of 15% oil-20% drug formulation with different amount of transferrin on the surface.

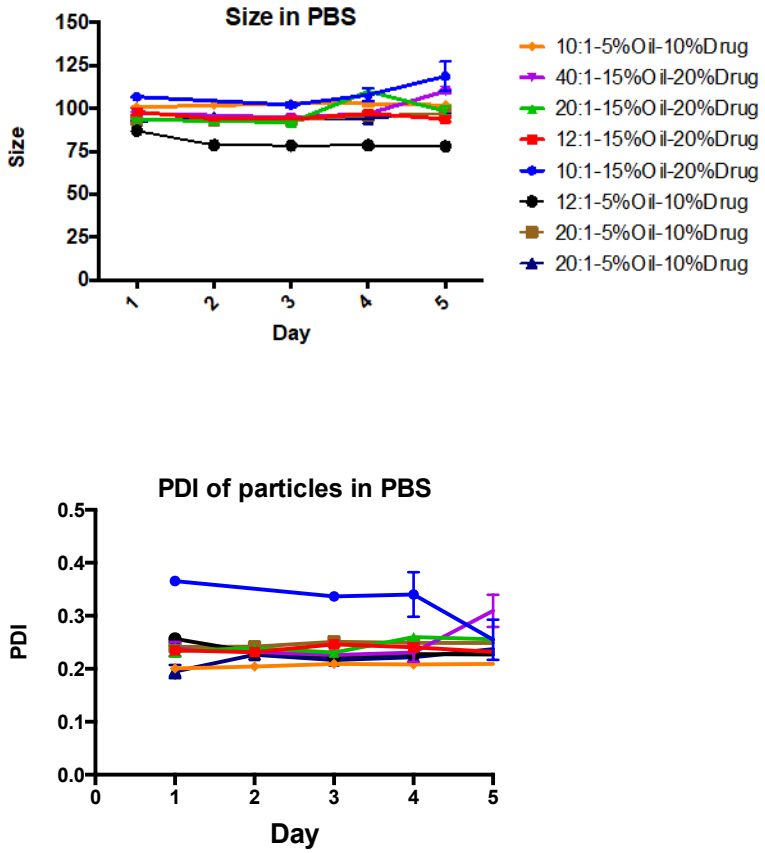

Figure 3.5 Size and PDI for different formulations in PBS stored at 37 ℃ for 5 days.

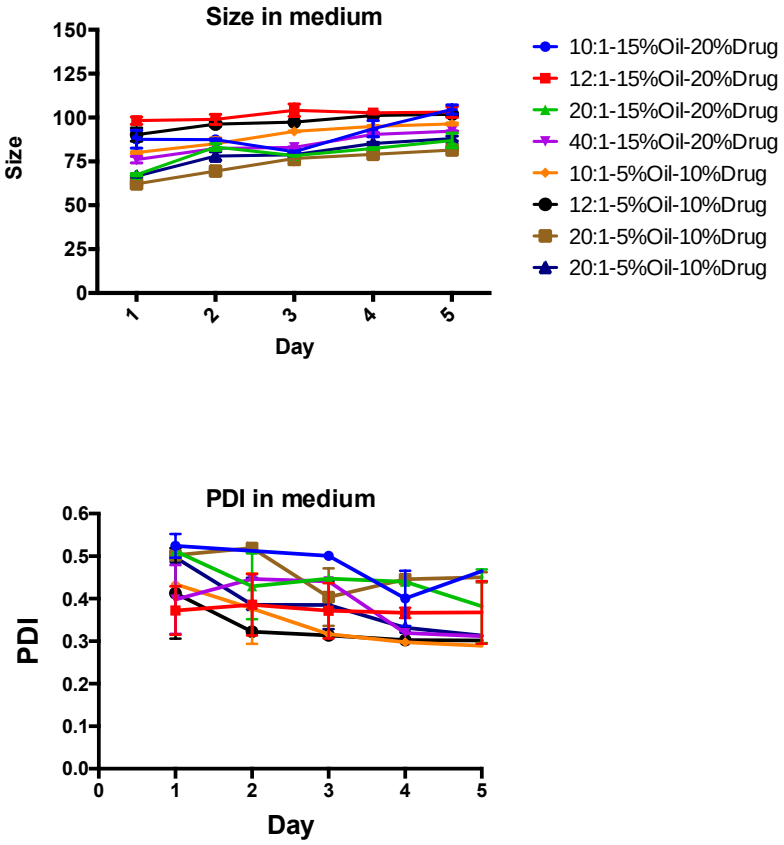

Figure 3.6 Size and PDI for different formulations in the cell culture medium stored at 37 ℃ for 5 days.

3.4.4. DSC and in vitro drug release

Solid lipid nanoparticle (SLN) is very similar to nanoemulsion in the way of components. Drug crystallization can be found a lot in SLN systems. This can lead to a burst release of the drug. Even though burst release is desirable in a few exceptional cases (like local wound treatment or pulsatile release), it is often unpredictable and difficult to control. Hence, it is generally considered as a negative phenomenon.[131] It leads to high local or systemic toxicity and is economically wasteful. As most of the drug is released in the initial minutes or hours it may result in therapeutic failure as no sustained release effect is achieved.[131, 132] The advantage of our Tf-NE-DRV is drug should be dispersed well in the oil core to avoid burst release. DSC and *in-vitro* drug release studies were performed to investigate the hypothesis.

TEM study was performed to check the drug dispersion inside the nanoemulsion system. The melting point of darunavir in the crystal form is 75℃, and this was confirmed in Figure 3.7(A). Tf-NE-DRV was the sample group, Tf-NE was the negative control, and the physical mixture of all the components was a positive control. No peak was detected at 75℃ for all three groups. In the positive control group, darunavir was immediately dissolved in DHA even though the nanoemulsion was not fabricated. In summary, no crystallization was observed in Tf-NE-DRV.

In-vitro drug release study was performed to investigate the drug release behavior further. As we can see from figure 3.8A, the desired sustained drug release was achieved. The overlap of the release curve for samples with and without transferrin revealed that this

amount of transferrin didn't affect the release. The free drug was released entirely within 6 hours while it took 32 hours to release entirely for those two nanoemulsion groups. The starting darunavir concentration was 0.4 mg/ml for all three groups. Even with the help of 2% Tween 80, darunavir didn't completely dissolve in the free drug group. This delayed the free drug release, even though it was under sink condition.

A.

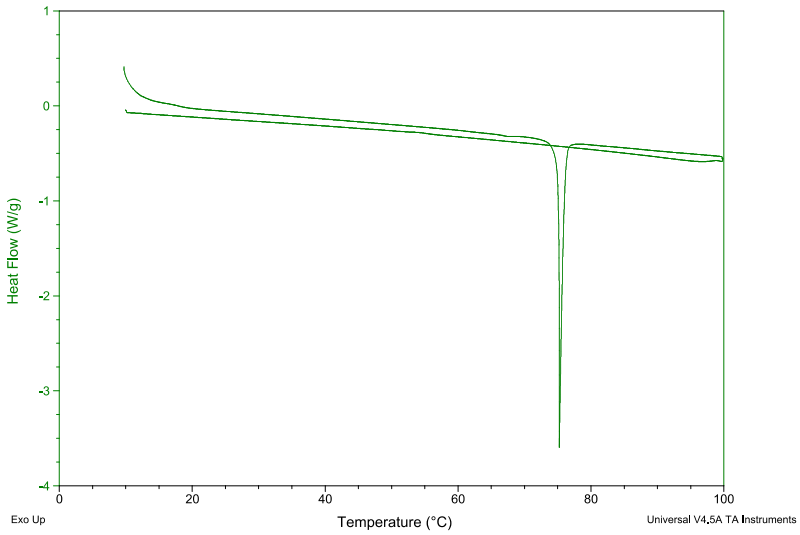

B.

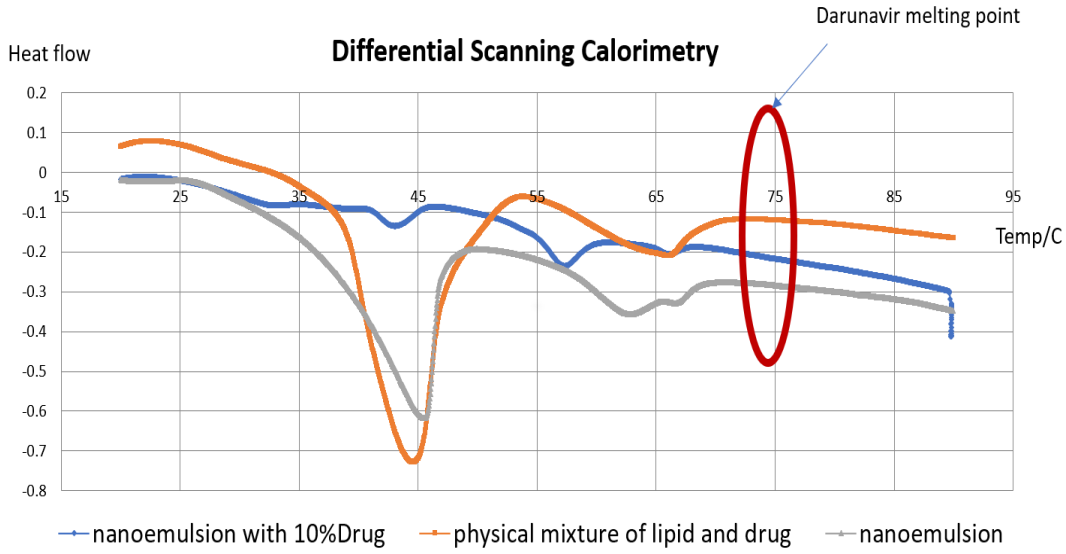

Figure 3.7 (A) Differential scanning calorimetry results of darunavir. (B) Differential scanning calorimetry results of different sample

A.

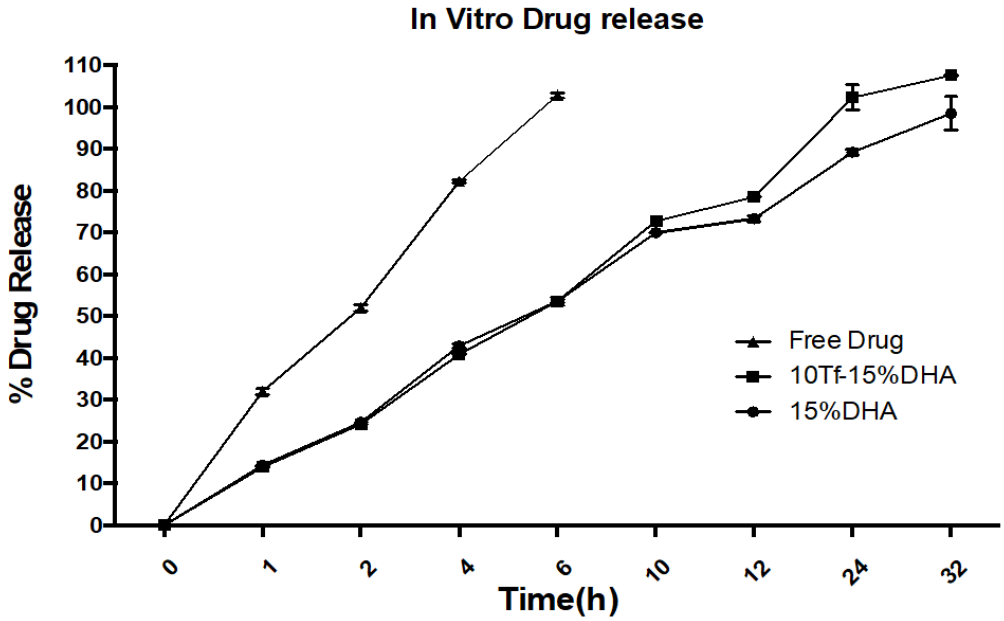

B.

Figure 3.8 (A) in-vitro drug release profile. (B) Illustration of drug release model.

3.5. Conclusion

The primary goal of this work was done develop a stable Tf-NE-DRV nanoemulsion system with decent drug loading and sustained release effect for highly lipophilic drug darunavir. Supported data shows that this is achieved. Our nanoemulsion system has proved to be successful in all the aspects including stability, high amount of drug encapsulation, even drug dispersion, and sustained drug release. Further in-vitro and in-vivo activities will be investigated in the following two chapters.

CHAPTER 4

IN VITRO ACTIVITIES OF Tf-NE-DRV

4.1. Abstract

In this chapter, our goal was to test the in vitro activity and brain delivery of Tf-NE-DRV. H-NMR was performed to test the DCM residual through preparation, and MTT studies were performed in different cell lines to test the safety of the nanoemulsion system. Cell update and drug transport studies were to demonstrate the brain delivery ability of Tf-NE-DRV. We used plasmid to successfully develop a lentiviral infected cell model, and we used this model to explore the anti-viral activity of Tf-NE-DRV. Surprisingly with a large amount of DHA in the system, NE-DRV was also able to achieve decent brain delivery without the help of transferrin. So, we explored more on the mechanism of NE-DRV brain delivery. Overall our nanoemulsions system Tf-NE-DRV was safe and able to achieve excellent brain delivery in *in-vitro* models. Tf-NE-DRV maintains the same therapeutic function as free drug darunavir in vitro.

4.2. Introduction

4.2.1. HIV-1 genome

Human immunodeficiency virus type 1 is a complex retrovirus encoding 15 distinct proteins, three polyproteins Gag, Pol and Env which are encoded by nine open reading frames, and six accessory proteins, Vif, Vpr, Vpu, Tat, Rev and Nef. The four Gag proteins include MA (matrix), CA (capsid), NC (nucleocapsid), and p6. Two Env

proteins are SU (surface or gp120) and TM (transmembrane or gp41). Gag and Env proteins are structural components that make up the core of the virion and outer membrane envelope. The three Pol proteins, PR (protease), RT (reverse transcriptase), and IN (integrase), provide essential enzymatic functions. HIV-1 encodes six additional proteins, often called accessory proteins, three of which (Vif, Vpr, and Nef) are found in the viral particle. Two other accessory proteins, Tat and Rev, provide essential gene regulatory functions, and the last protein, Vpu, indirectly assists in the assembly of the virion. [133] The genetic organization and structure of HIV-1is illustrated in Figure 4.1.

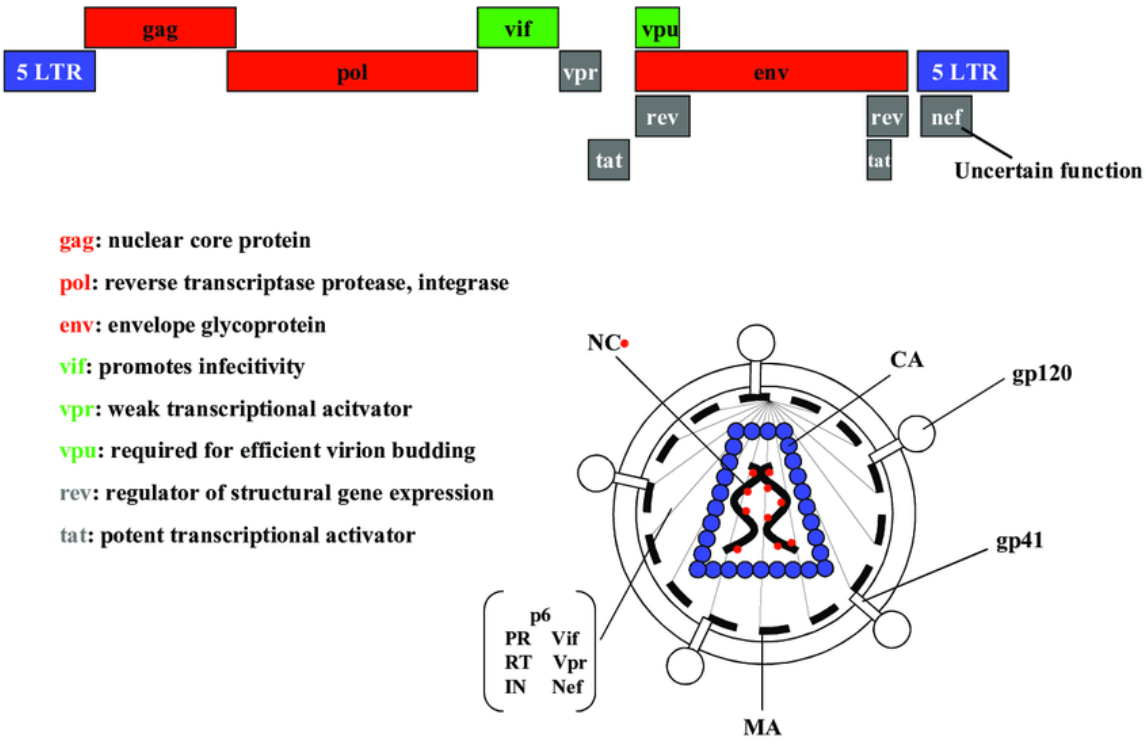

Figure 4.1 Genetic organization and structure of HIV-1

4.3. Experimental Section

4.3.1. Materials

hCMEC/D3 cell line was purchased from CELLutions Biosystems. The EndoGRO-MV culture media kit (5% serum) and Collagen type I (rat tail) were purchased from Millipore Sigma. 293T cell line was a gift from Dr. Wenhui Hu from Temple University, school of medicine. Dulbecco's Modified Eagle's Medium (DMEM) with10% fetal

bovine serum and 1% penicillin-streptomycin was used for 293T cell line. Lenti-X p24 Rapid Titer Kit was purchased from Clontech.

4.3.2. Cell culture

The hCMEC/D3 BBB cell line has been extensively characterized for brain endothelial phenotype and is a model of human blood-brain barrier (BBB) function.This cell line has transferrin receptor expression and is a suitable model for BBB transport and permeability studies[134]. For the hCMEC/D3 cell line, collagen was diluted into 150 ug/ml using RNase-free water. Before each cell passage, 3ml of collagen solution was added to 100mm Petri dish, which covered the whole bottom of the dish and incubated at 37℃ for 1 to 2 hours. Then this pre-coated dish was used for cell passage by following the standard steps. The transferred cells were incubated in 5% CO^2 at 37 ℃. Cells need to be passaged every other day.

For 293T cell line, trypsinized cells were transferred to a new petri dish and incubated in 5% CO^2 at 37 ℃. Cells also need to be passaged every other day.

4.3.3. Brain cell viability

MTT assays were performed to evaluate the Tf-NE-DRV toxicity in the hCMEC/D3 cell line. Subconfluent cells were seeded in 96-well microplate and allowed to attach under standard cell culture conditions. After 24 h, Tf-NE-DRV (5nM to 75uM in darunavir concentration) was added to the wells and incubated for 24 h at 37 ºC. Tf-NE was used as a negative control while free darunavir served as negative control. After 24 h, 20 µl of 5

mg/mL 3-(4,5-dimethylthiazol-2-yl)-2,5-diphenyltetrazolium bromide (MTT) reagent was added to the wells and allowed to incubate for 2 h. At the end of 2 h, the medium was discarded. To each well, 150 µl of DMSO was added to dissolve the purple formazan dye produced by the metabolically active cells. The UV absorbance of the colored dye produced was measured at 560 nm. Untreated cells served as a baseline control.

4.3.4. Cell uptake using fluorescent microscopy

To study whether Tf-NE-DRV can get into the brain through the transferrin receptor, cell uptake studies were carried out using fluorescent microscopy. 18:1 Liss Rhod PE (1,2-dioleoyl-sn-glycero-3-phosphoethanolamine-N-(lissamine rhodamine B sulfonyl) (ammonium salt)) was inserted into the systems as a fluorescent label.

hCMEC/D3 cells were seeded to 100mm Petri dishes with coverslips at the bottom for two days. The cells grew and formed a single layer on the coverslips. Then each coverslip was transferred to a 30mm Petri dishes and 3mL Tf-NE-DRV sample, which consisted 1ml Tf-NE-DRV suspension and 2ml cell culture medium (1mg/ml final concentration), was added to the same petri dish. Samples were put back to incubation at 37 ℃ for 4 hours. 3ul DRAQ5 fluorescent probe solution (5mM) was added to each dish for cellular staining 15mins before the incubation ended. Coverslips were very gently washed at least 3 times using DPBS buffer before imaging. In this study, NE-DRV was used as a negative control. Tf-NE-DRV samples with 4 different amounts of transferrin including 10:1, 12:1, 20:1 and 40:1 were tested. (Rhod PE: Ex=560nm / Em=583nm; DRAQ5: Ex=646nm / Em=681nm)

4.3.5. Western blot analysis

The cells were harvested with M-PER Mammalian Protein Extraction Reagent (Pierce, Rockford, IL) supplemented with 0.2% v/v protease inhibitor cocktail P8340 (Sigma–Aldrich, St. Louis, MO). Aliquots of cell lysate were resolved on 8 % SDS-polyacrylamide gel (25 μg protein loading per lane) and electrotransferred onto a polyvinylidene difluoride (PVDF) membrane (Immobilon-P 0.45 μm, Millipore, Billerica, MA). Membranes were blocked with Tris-buffered saline containing 0.1% Tween 20 and 5% dry skim milk powder. Transferrin receptor and β-actin were detected with mouse CD71 monoclonal antibody (1:1000) and β-actin antibody (1:5000 dilution) respectively, followed by anti-mouse IgG (1:10000) as secondary antibodies. Proteins were visualized using enhanced chemiluminescence according to the manufacturers' instructions (Pierce, Rockford, IL).

4.3.6. Drug transport

To study the CNS targeted and transport activity of Tf-NE-DRV, drug transport assay was performed. The BBB model was established using Transwell Permeable Supports in Figure 4.2. Collagen was used to pre-coat the PET cell culture inserts for at least 1 hour, followed by multiple washes using DPBS before seeding the hCMEC/D3 cells. The plate was incubated at 37℃ until confluent cell monolayer formed.

To start the assay, Rhod labeled Tf-NE-DRV was added to the apical side, and fresh medium was added to the basolateral side. Lucifer yellow was added to each well to monitor the integrity of the confluent cell monolayer. The plate was incubated at 37℃

for 6 hours, and the 150ul sample was taken out at a certain time point (1hr and 6hr). The same amount of fresh medium was put back. Results were measured spectrometerly. (Rhod PE: Ex=560nm/Em=583nm, Lucifer yellow: Ex=428nm/Em=536nm).

A.

B.

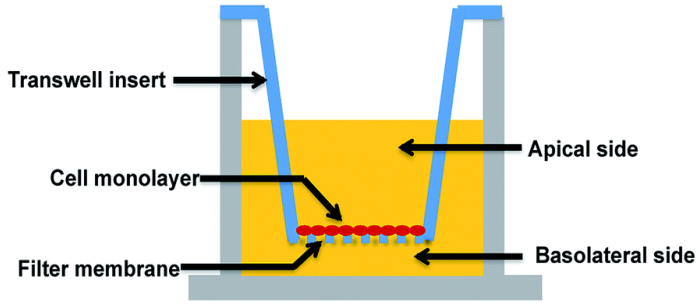

Figure 4.2 (A) Transwell Permeable Supports. (B) Cross-section illustration of the model.

4.3.7. Establishment of the in-vitro disease model

Due to the biosafety regulation, we can't directly use HIV infected cells to study efficacy. Instead, we developed an in vitro disease model using lentivirus. Viral production schematic is showed in Figure 4.2. Packaging vector, pCl-ECO plasmid, provided gag-pol polyprotein and the pCMV-VSV-G plasmid was used as envelop vector. Same as the schematic, GFP expression plasmid DNA was used as a transfer vector. The mixture of these three plasmids was added to the target cells, and transfection was conducted using the calcium chloride transfection method. Darunavir is a protease inhibitor, which targets pol protein. With the essential structural proteins and targeted proteins, this lentiviral particle is sufficient to be an in vitro infection model for study.

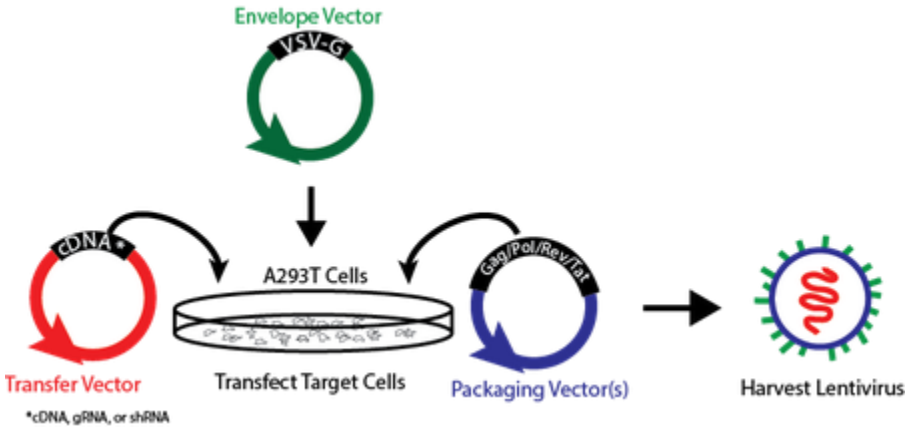

Figure 4.3 Viral production schematic. (From www.addgene.org)

4.3.8. In vitro anti-HIV activity

Infected cell model was established using 293T cells as the method described in 4.3.7. Tf-NE-DRV was used to treat the infected cells in different concentrations. Free darunavir was used as a positive control while Tf-NE was used as negative control. After treatment, the supernatant was collected from each sample. The viral concentration of the supernatants was measured using the Lenti-X p24 Rapid Titer Kit. The fluorescent label GFP was co-transfected into the cells. So successfully transfected cells can be visualized under fluorescent microscopy. Titer can also be calculated by directly counting the number of infected cells.

4.3.9. Statistical analysis

The results are expressed as means ± SD. The significance of differences was assessed using a t-test, and $p<0.05$ was considered significant unless otherwise specified.

4.4. Results and discussion

4.4.1. Toxicity

During the preparation of Tf-NE-DRV, DCM was used as a solvent, which is detrimental to human health. To make sure there was no DCM residual in the system, NMR was performed. DMSO was the solvent. From figure 4.4, we didn't see any peak at 5.76, which suggested DMC residual was under the detection limit.

MTT assay was performed in hCMEC/D3 and 293T cell lines to investigate the toxicity of Tf-NE-DRV. Results were summarized in Figure 4.4. Tf-NE-DRV, Tf-NE, and

darunavir were used to treat the hCMEC/D3 cells at a wide range of drug concentration from 0.2uM to 60mM. In 293T cells, two samples, Tf-NE-DRV, and darunavir were used as treatment from 0.64nM to 400nM. As we can see from the graphs, cell viability maintained around 100% as concentration increased for all groups. In summary, both our nano carrier system and darunavir showed no toxicity.

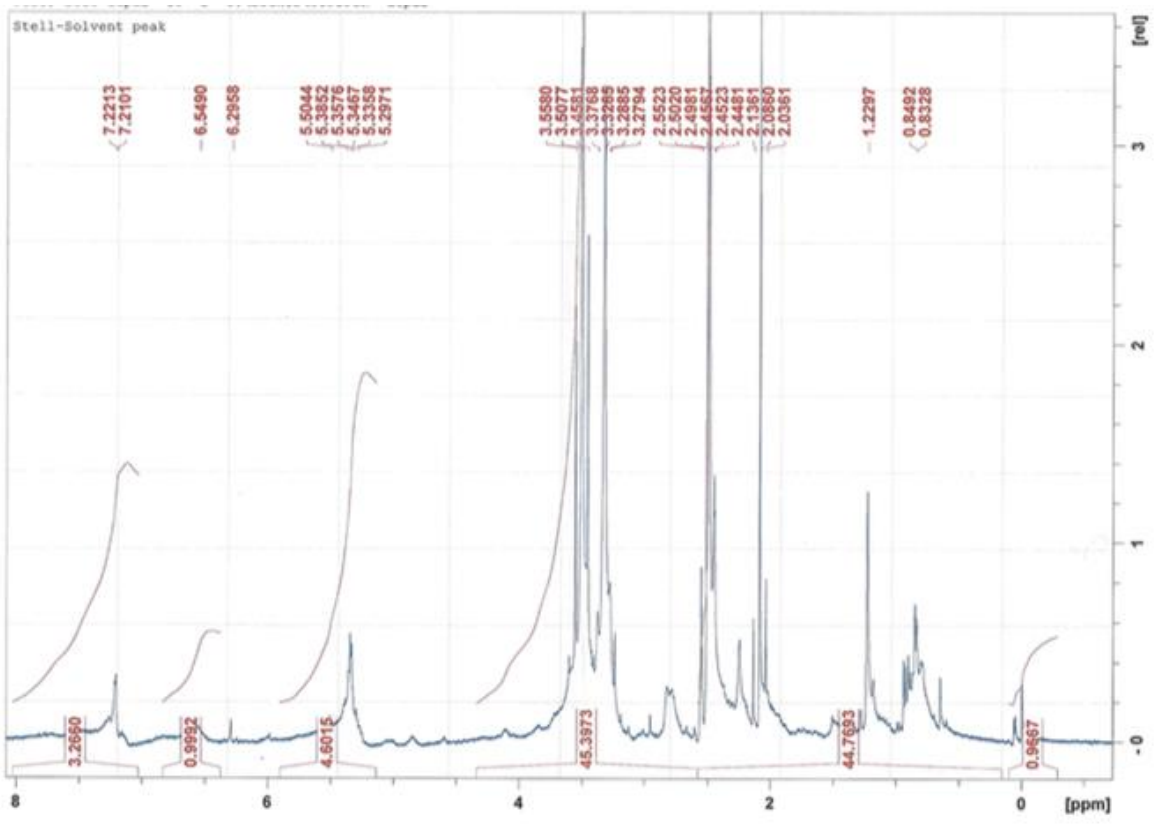

Figure 4.4 NMR of lyophilized Tf-NE-DRV; DMSO was used as the solvent.

A.

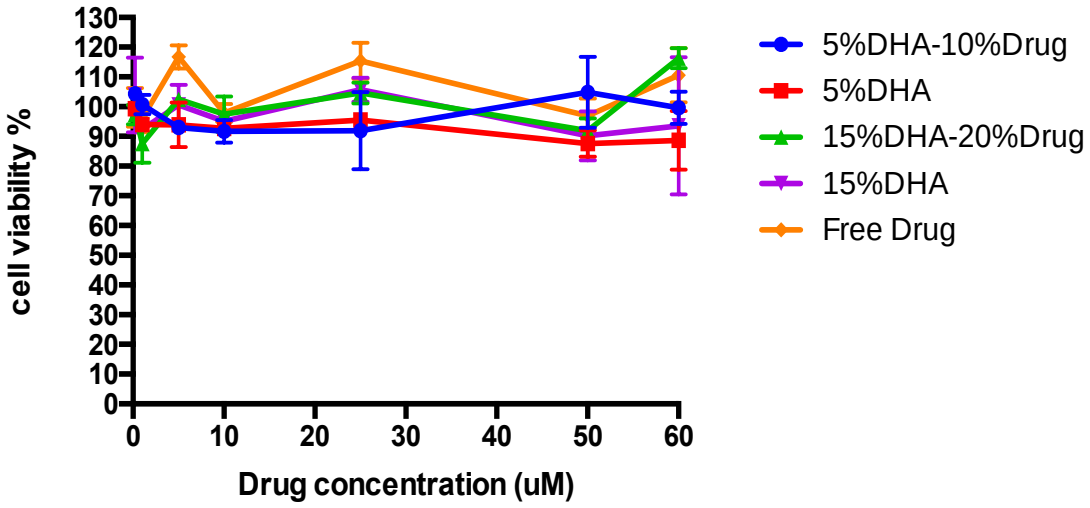

B.

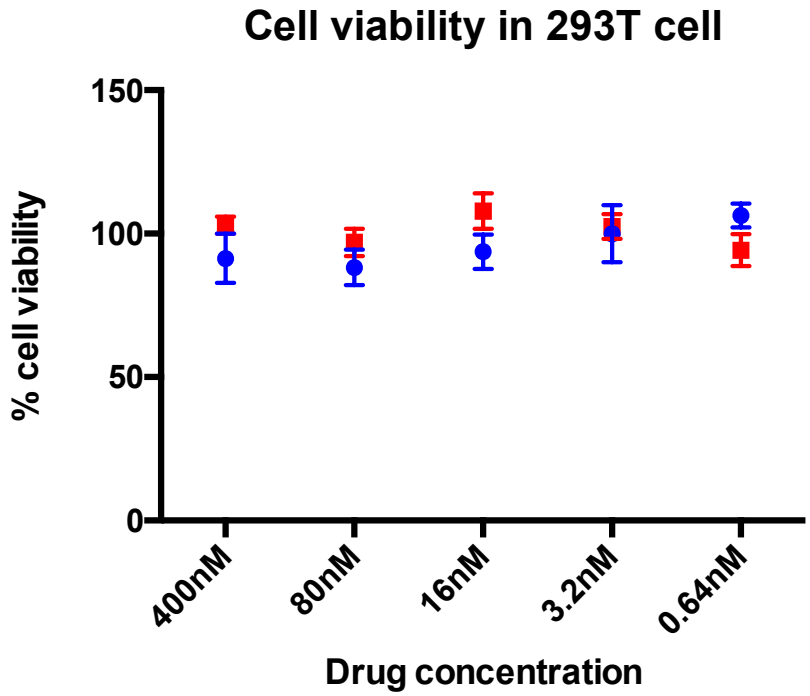

Figure 4.5 (A) hCMEC/D3 cell viability, (B) 293T cell viability, Blue is darunavir and red are Tf-NE-DRV.

4.4.2. CNS targeting, uptake and transport activities

The CNS targeting activity was investigated using the hCMEC/D3 cell line. The hCMEC/D3 BBB cell line has been extensively characterized for brain endothelial phenotype and is a model of human blood-brain barrier (BBB) function.[134, 135] As we know from the reference, there is transferrin receptor expression in this cell model. Western blot was performed to confirm that. The result was presented in Figure 4.6. A prostate carcinoma cell line named PC-3M, which has CD71 overexpression was used as a positive control.

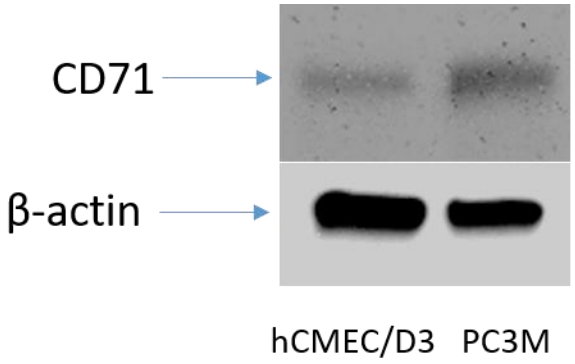

Figure 4.6 Western blot against the transferrin receptor (CD71)

Uptake study was carried out between 2 different Tf-NE-DRV formulations, which contains 5% DHA and 15% DHA respectively. NE-DRV was used as negative control. The results in figure 4.6 can be separated into two groups based on the formulation. Let's look at the left part, which was the results for 5% DHA Tf-NE-DRV. No uptake happened without transferrin as shown in the control graph. But in the samples with transferrin, we can see uptakes. No noticeable difference in uptake was observed in samples with different amount of transferrin. We can summarize that Tf-NE-DRV can successfully achieve CNS through the transferrin receptor. Then we move to the 15% DHA Tf-NE-DRV, we can see stronger cell uptake from sample groups with transferrin. But surprisingly, the 15% DHA control group also had a decent amount of uptake. The only difference between these two groups was the DHA amount, which makes us wonder if DHA can help the CNS targeting. This discovery drove the project in an exciting direction.

To investigate the drug transport activity of our formulations and to deeper explore the DHA's role in CNS targeting as well, drug transport assay was performed using the hCMEC/D3 cell line. Tf-NE-DRV and NE-DRV were the sample groups, and darunavir free drug was the negative control. The results were summarized in Figure 4.8. At 1 hour, Tf-NE-DRV had significantly better drug transport results compare to free drug darunavir while NE-DRV has similar results as free drug. But at 6 hours, both formulation groups showed significantly better results than the free drug. By comparing these two formulation groups, Tf-NE-DRV was slightly better than NE-DRV in the performance of

drug transport. Lucifer yellow is a fluorescent marker which has been widely used as a reference or indicator of the tight junction of the BBB model. During our studies, Lucifer yellow was added to each sample for monitoring. P values of all the groups were smaller than 21.7e-6, [136] which indicated the integrity of the BBB tight junctions.

From the result, we can see 15% DHA NE-DRV without transferrin can achieve good cell uptake and drug transport results. Even though it had a slow onset of drug transport and the performance was slightly below compared to Tf-NE-DRV. The omission of the targeting moiety will significantly decrease the complexity of systems and bring enormous advantages for manufacturing. Therefore, we explored more on the DHA CNS targeting mechanism and results were discussed in 4.4.4.

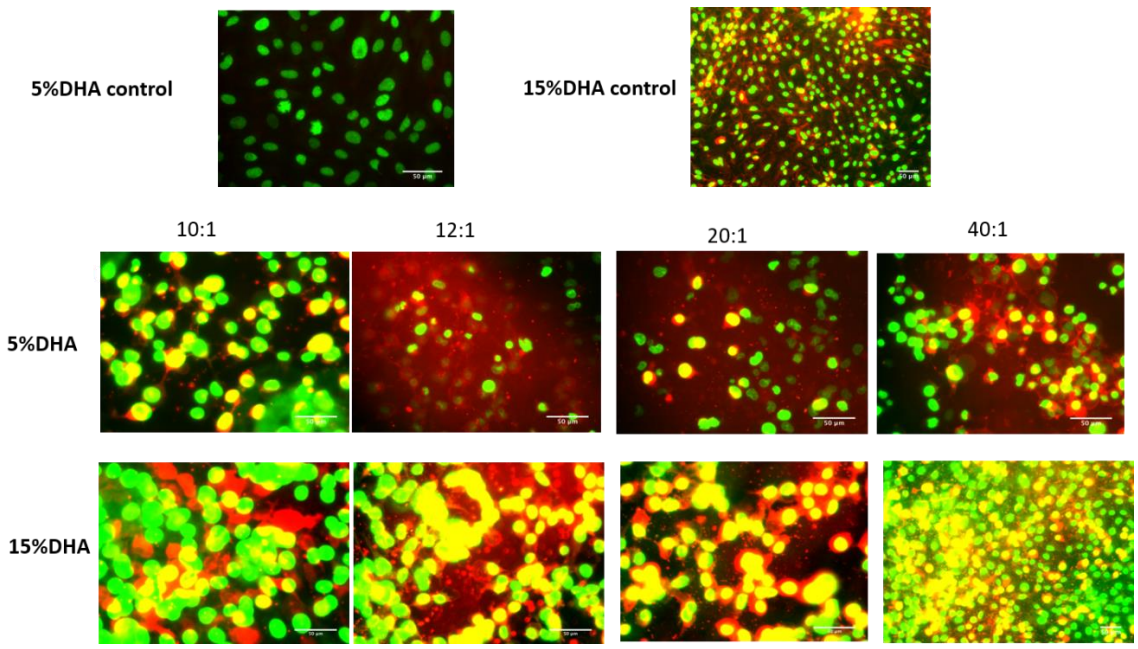

Figure 4.7 Cell uptake results. 10:1, 12:1, 20:1 and 40:1 were different lipid-to-transferrin weight ratios. Cellular was labeled in green. Tf-NE-DRV or Tf-NE were labeled in red. The overlap of cellular and nanoemulsion system appeared yellow. 5% DHA control is NE-DRV with 5% DHA; 5% DHA is Tf-NE-DRV with 5% DHA and different amounts of transferrin. 15% DHA control is NE-DRV with 15% DHA; 15% DHA is Tf-NE-DRV with 15% DHA and different amounts of transferrin.

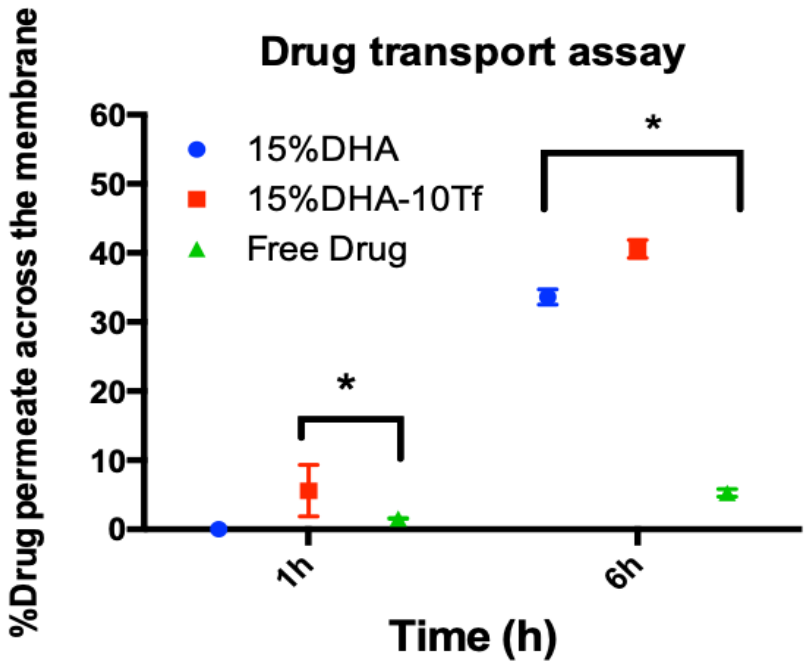

Figure 4.8 Drug transport assay result Blue is 15% DHA NE-DRV; Red is 15% Tf-NE-DRV; Green is darunavir. * $p<0.05$ comparing 15% DHA Tf-NE-DRV and free drug at 1 hour; $p<0.05$ comparing all three groups at 6 hours

4.4.3. Anti-viral activity

NE-DRV was used here as a treatment since transferrin is not going to help in this study. Free drug darunavir was positive control, and NE (nanoemulsion without drug encapsulation) was used as negative control. Solvent affection was excluded. From the cell viability results we discussed in 4.4.1, we are sure that our nanosystem is safe and won't cause any 293T cell death. Furthermore, all the anti-viral activity was from darunavir. Cells were treated with three different concentrations, 50nM, 100nM, and 200nM. Considering the IC50 of darunavir, we overdosed the samples. But the linear range of the ELISA (enzyme-linked immunosorbent assay) kit was narrow, and due to the limited amount of time I had, we didn't optimize the transfection process and treatment concentration. We did notice that the cell vitality will affect the transfection result. If the cell were confluent on the petri dish, they tend to be less dynamic, and the titer will be lower. But if the cells were at the active differentiation stage, we will get extremely high viral concentrations.

All we are trying to see if the formulation won't change the anti-viral activity of darunavir and the NE-DRV can at least achieve the same therapeutic results. Of course, we can see almost complete viral inhibition from Figure 4.9 through the p24 ELISA method. GFP was co-transfected into the cells. So, cells were able to be visualized under a fluorescent microscope if they were infected. Pictures were taken and illustrated in Figure 4.10. In order to confirm the p24 ELISA results, the titer calculation method was also employed to get the efficacy result by using these pictures (Figure 4.11). The results were in very good accordance with ELISA.

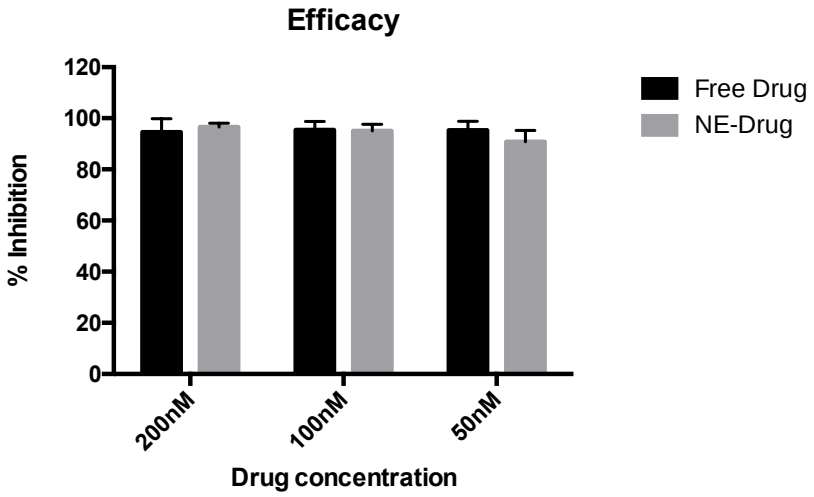

Figure 4.9 Efficacy result based on the titer from P24 Elisa

A.

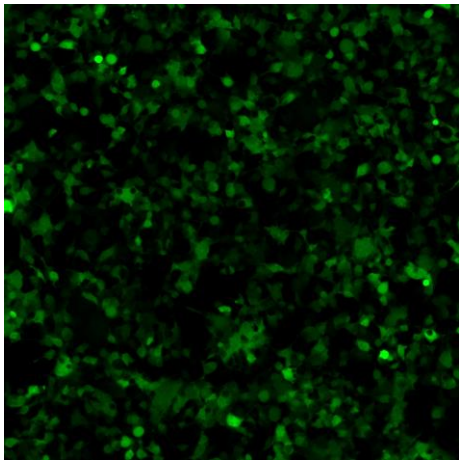

B.

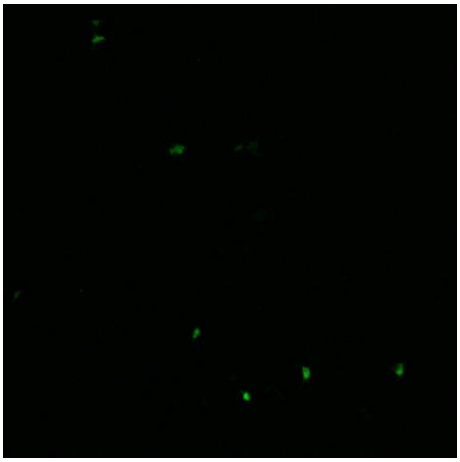

Figure 4.10 (A) the fluorescent picture of NE (negative control group); (B) the fluorescent picture of NE-DRV (treatment group)

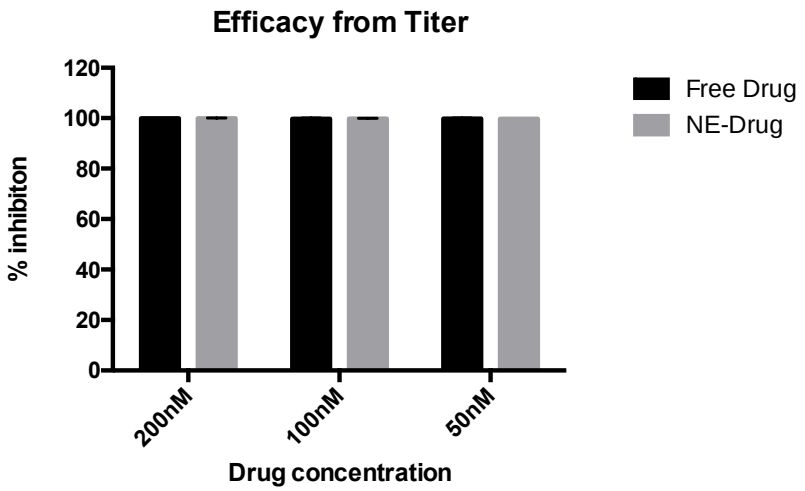

Figure 4.11 Efficacy result based on calculated titer from GFP expression

4.4.4. DHA associated CNS targeting mechanism

DHA is an omega-3 fatty acid that is essential for healthy brain growth and cognitive function.[137, 138] Consistent with its importance in the brain, DHA is highly enriched in brain phospholipids.[139, 140] However, DHA cannot be de novo synthesized in the brain and must be imported across the blood-brain barrier. Recently, major facilitator superfamily domain-containing protein 2 (Mfsd2a) was found to be the major transporter for DHA uptake into the brain.[141] So I proposed the DHA related CNS targeting was associated with mfsd2a transporter.

Msfd2a is critical for the formation and function of the BBB. [143] Western blot proved that there was mfsd2a expression in the hCMEC/D3 cell line. I tried to develop a mfsd2a knockdown cell model using siRNA silencer to investigate the DHA related CNS targeting mechanism. By following the protocols from the manufacturer, cells were treated with siRNA for once, twice and three times and western blot was performed to investigate the protein expression change. As we can see in Figure 4.12, we didn't successfully knockdown any expression even after three times of treatment. According to the reference lipofectamine 2000 has good transfection efficiency with hCMEC/D3 cell line. Knockdown the protein does not always follow the knockdown at the mRNA level, some proteins are very stable, and reduction at the protein level may not be seen.

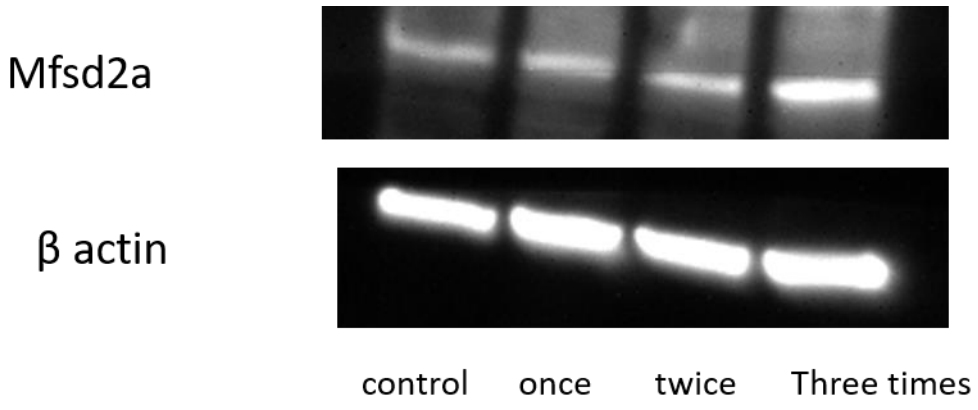

Figure 4.12 Western blot results of siRNA knockdown study

As we didn't successfully develop a mfsd2a knockdown cell model, we try to find a blocker of mfsd2a instead. But this receptor is not well characterized, and not much information was obtained from literature research. However, tunicamycin, which is a mixture of homologous nucleoside antibiotics, has been confirmed to be uptake by mfsd2a[142]. So, we did the cell uptake again with the co-treatment of NE-DRV and tunicamycin in the hCMEC/D3 cell line. There was big limitations in this model. We weren't sure if the NE-DRV and tunicamycin were going to compete with each other. But it worth a try to gather more information. The results are shown in Figure 4.13. As the concentration of tunicamycin increased, the NE-DRV uptake was increased, which is contrary to our hypothesis. It seems mfsd2a transporter is not involved in the NE-DRV brain uptake process.

We did the permeability studies again in the Caco-2 cell line, and the results were presented in Figure 4.14. Without mfsd2a expression in Caco-2, NE-DRV can transport a very good amount of drug across the membrane compared to free drug ($p>0.05$) over 6 hours.

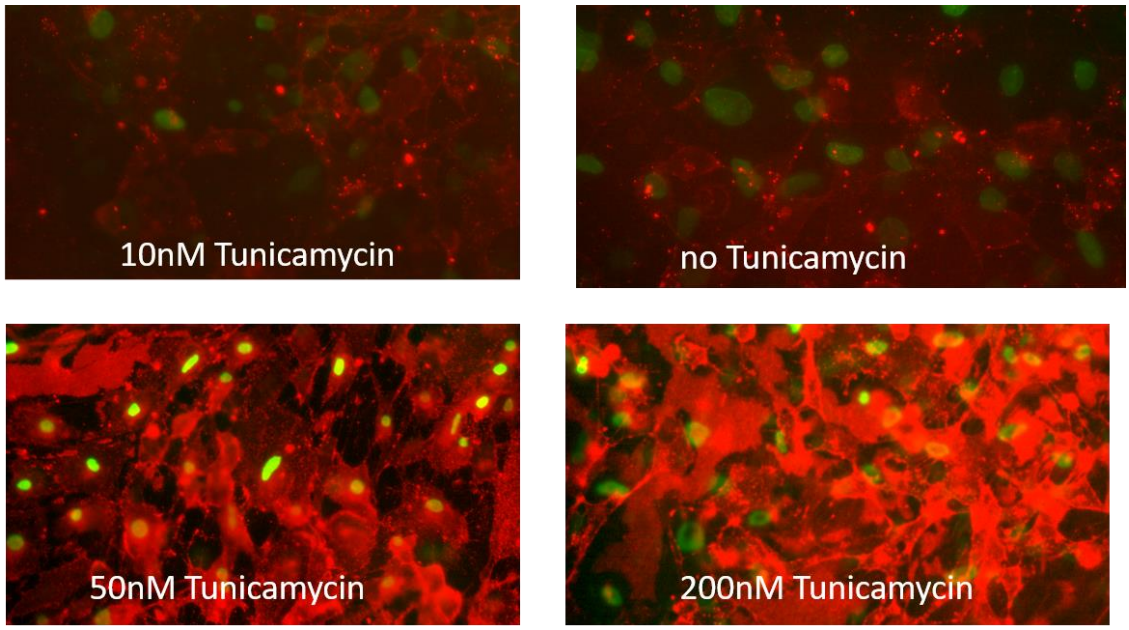

Figure 4.13 Cell uptake results with the different amount of Tunicamycin under a fluorescent microscope. Red: NE-DRV; green: Nucleus.

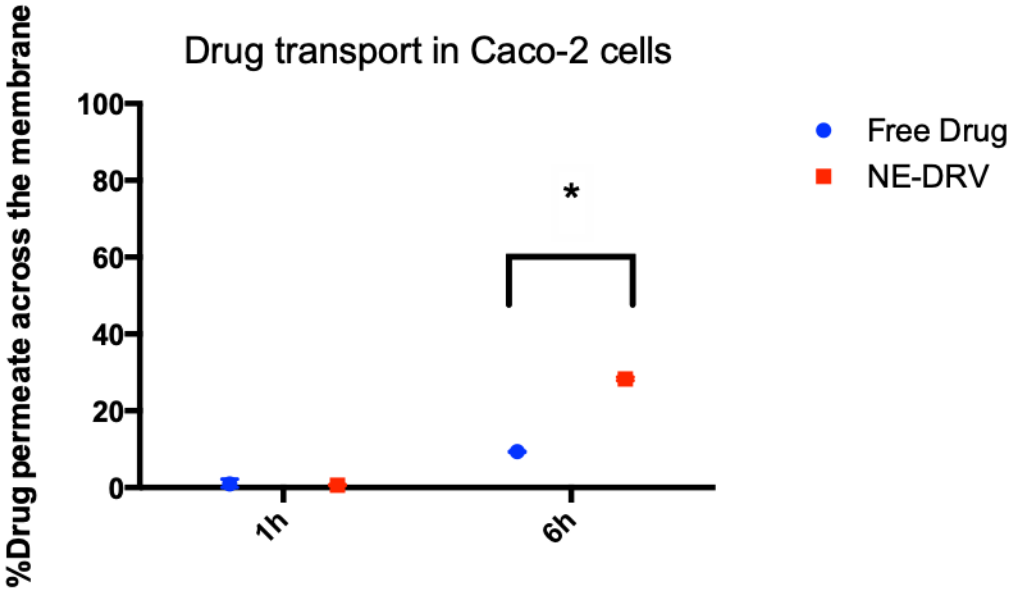

Figure 4.14 Drug transport study in Caco-2 cell line

4.5. Conclusion

In this chapter, our goal was to test the in vitro activity and brain delivery capability of Tf-NE-DRV. Firstly, we have to make sure the system itself is safe to the human body. Although the preparation process introduced organic solvent DCM into the system, which is toxic. H-NMR result showed there was no residual existing in prepared Tf-NE-DRV. Our nanoemulsion system also has been proved to be safe to human cells through viability studies in different cell lines. Cell update and drug transport studies demonstrated the brain delivery ability of Tf-NE-DRV. Surprisingly with a large amount of DHA in the system, NE-DRV was also able to achieve decent brain delivery without the help of transferrin. So, we explored more on the mechanism of NE-DRV brain delivery. Finally, we demonstrated that the DHA of NE-DRV can better solubilize the drug and improve the permeation. We used lentiviral successfully created a disease cell model. Tf-NE-DRV was proved to have a good anti-viral activity as the free drug darunavir in vitro.

Overall, Tf-NE-DRV maintained its therapeutic function, successfully passed the BBB and increased the darunavir brain concentration in vitro.

CHAPTER 5

IN VIVO BIODISTRIBUTION OF Tf-NE-DRV AND FUTURE DIRECTIONS

5.1. Abstract

We explored the in vivo biodistribution of Tf-NE-DRV in healthy mice. Ex vivo imaging study and biodistribution study were performed to explore the brain delivery ability of our nanoemulsion system. Based on the results, we can come to the conclusion that both Tf-NE-DRV and NE-DRV can improve brain delivery of DRV and the concentration was close to the therapeutic concentration of DRV. Conclusion and future directions were discussed in this chapter.

5.2. Experimental Section

5.2.1. Materials

1,2-distearoyl-sn-glycero-3-phosphocholine (18:0 PC, 850365), 1,2-distearoyl-sn-glycero-3-phosphoethanolamine-N-[methoxy(polyethylene glycol)-2000] (ammonium salt) (18:0 PEG2000 PE, 880120), 1,2-distearoyl-sn-glycero-3-phosphoethanolamine-N-[maleimide(polyethylene glycol)-2000] (ammonium salt) (DSPE-PEG(2000) Maleimide, Avanti, 880126), Cholesterol were all purchased from Avanti Polar Lipids, Inc. Darunavir (SML0937) was purchased from Sigma-Aldrich. DiR (1,1'-Dioctadecyl-3,3,3',3'-Tetramethylindotricarbocyanine Iodide) was purchased from Thermo Fisher. BALB/c male mice were purchased JAX laboratory.

5.2.2. Ex vivo Imaging study

Six mice were randomly separated into three different groups. They were a vehicle control group, Tf-NE-DRV group, and NE-DRV group. 0.6% w/w DiR was added to the nanoemulsion systems as a fluorescent label. After certain days of dosing, mice were sacrificed, and organs were harvest for imaging. Odyssey® CLx Infrared Imaging System from LI-COR was utilized to get the imaging.

5.2.3. In vivo biodistribution study

The experimental protocol of the in vivo biodistribution study was approved by the IACUC. The drug biodistribution was conducted in compliance with the guidelines. 30 mice were randomly separated into 10 groups. They were control vehicle group, 3 day consecutive doses of Tf-NE-DRV group, 3 day consecutive doses of NE-DRV group, 3 day consecutive doses of free drug, 2 day consecutive doses of Tf-NE-DRV group, 2 day consecutive doses of NE-DRV group, 2 day consecutive doses of free drug, one dose of Tf-NE-DRV group, one dose of NE-DRV group, one dose of free drug. Mice were sacrificed after and organs were harvested. Tissues were homogenized to measure the drug concentration using the LC-MS.

5.3. Results and discussion

Both NE-DRV and Tf-NE-DRV can successfully enter the brain. In the treatment groups, we can see distinctly brighter green signal in brain tissues after 3-day dosing compared to control groups (Figure 5.1). From the biodistribution data in Figure 5.2, brain drug concentration was significantly increased to reach the IC50 of darunavir which is about

5nM after 2-day consecutive dosing. Furthermore, the concentration of darunavir maintained in the brain for day 3. There was no a significant difference between Tf-NE-DRV and NE-DRV. From Figure 5.3 we can see that liver and spleen retained most of the doses. Biodistribution results (Figure 5.4) were in good accordance with the imaging results. This indicated that formulation is not stable enough inside the human body and the particle size grew before or after injection. We are doing at 10mg/kg drug concentration, which leads to an extremely high lipid concentration. This could be a potential reason for instability.

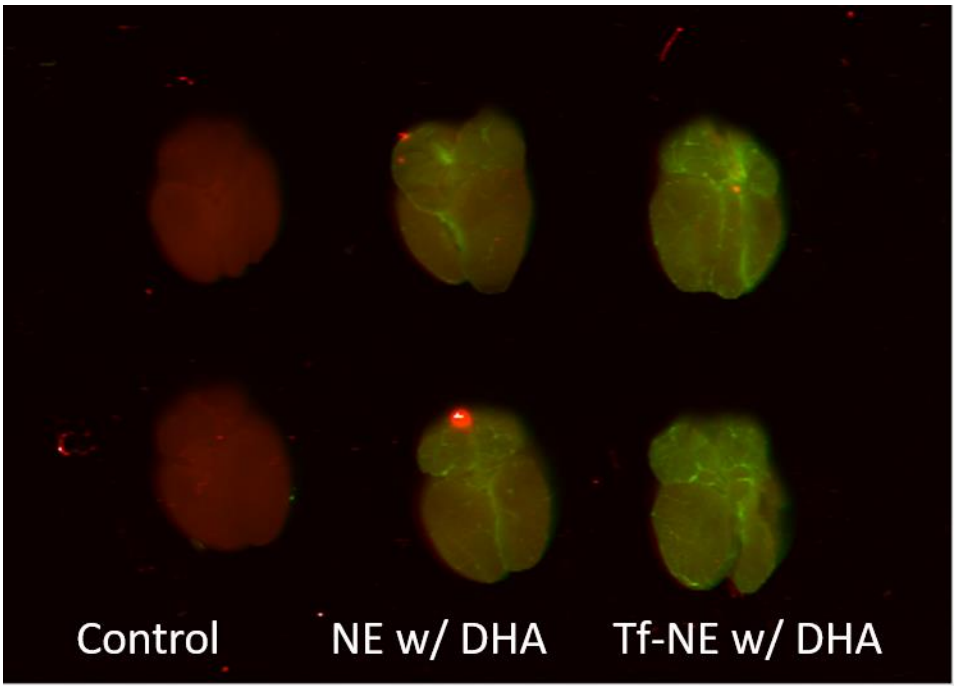

Figure 5.1 Imaging of the brain after 3 days injection; Red is brain tissue; Green was nanoemulsion systems.

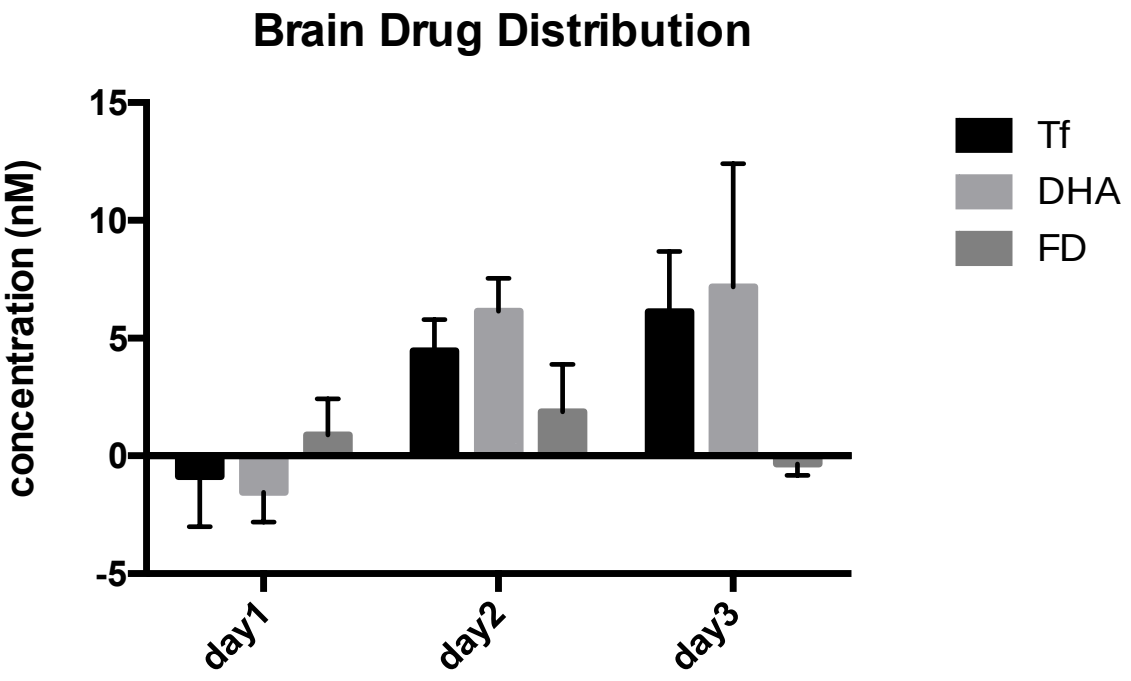

Figure 5.2 Drug concentration in brain tissues. Black is Tf-NE-DRV, light grey is NE-DRV, grey is free drug darunavir

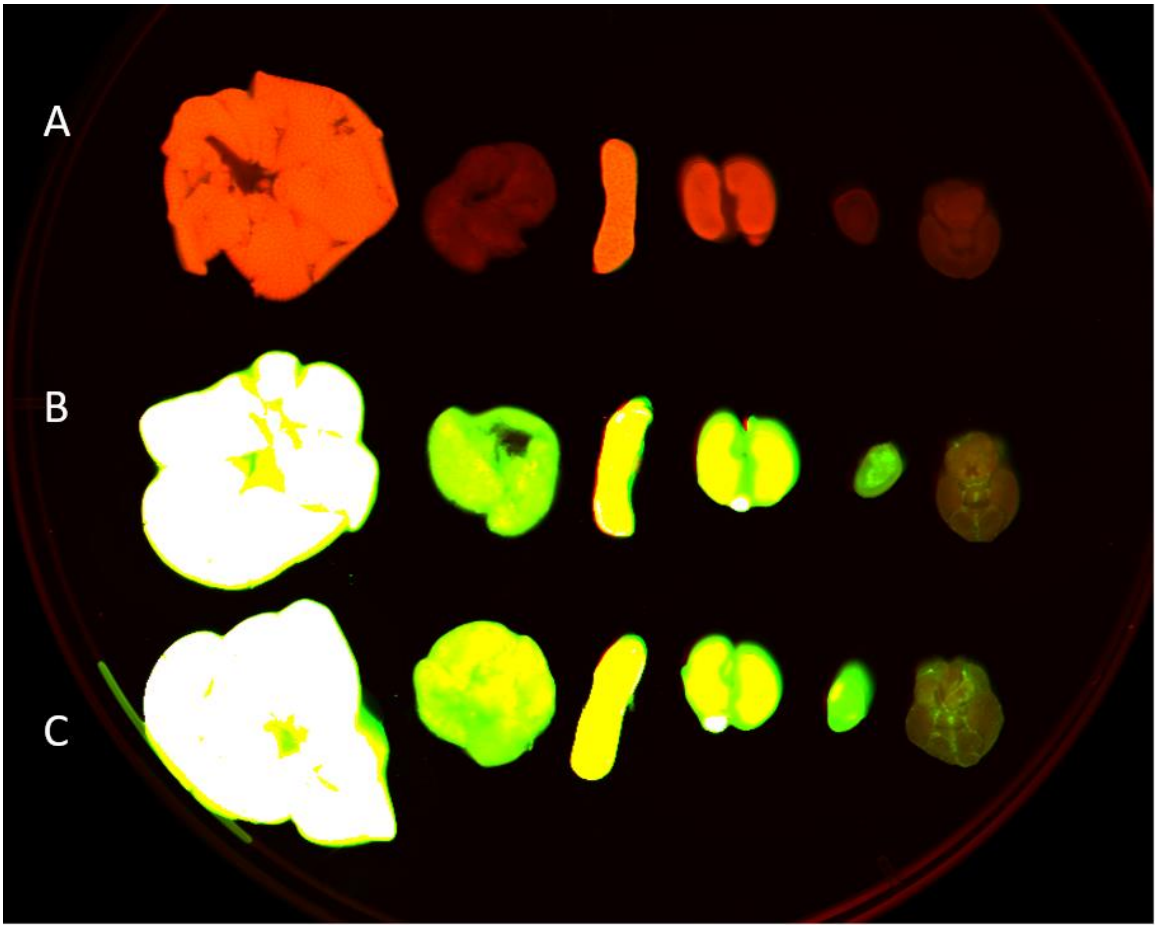

Figure 5.3 Imaging of major organs after 3 days injection. A: vehicle group; B. NE-DRV group; C. Tf-NE-DRV group. Organ tissues were in Red; nanoemulsion systems were in green. Organs are liver, lung, spleen, kidney, heart and brain.

A.

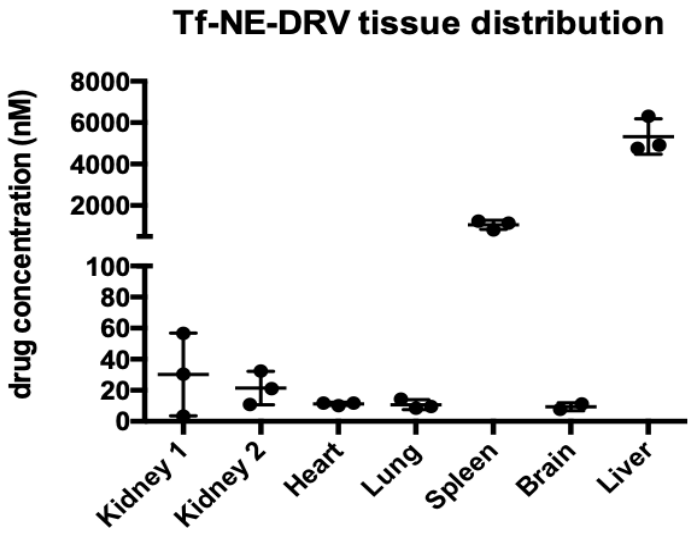

B.

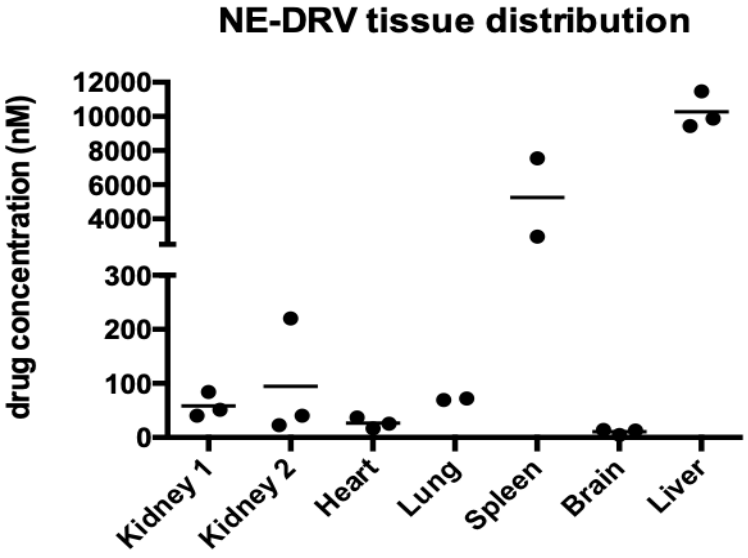

Figure 5.4 A. Biodistribution of darunavir after 3-day consecutive dosing of 10mg/kg Tf-NE-DRV; B. Biodistribution of darunavir after 3-day consecutive dosing of 10mg/kg NE-DRV

5.4. Summary

The main goal of this work was to develop a brain targeted nanoemulsion system to improve the brain delivery of antiretroviral drugs.

In the formulation part, we chose the most appropriate stabilizer cholesterol and oil DHA to form our Tf-NE-DRV. Although tripalmitin worked slightly better than cholesterol as a stabilizer by looking at the particle sizes. Small size represents that the lipids are better aligned and packed. The nanoparticles were more rigid and compact in this case. But rigidity is not always a useful feature for nanoparticles, and you have to take different applications into consideration. [125] Soft nanoparticles tend to escape more from the RES system. Transferrin coupling is very efficient using the NHS ester crosslinking method. There was no significant difference between different sample groups.

Tf-NE-DRV nanoemulsion systems were successfully developed with a decent drug loading (12%) and sustained release profile for highly lipophilic drug darunavir. Supported data showed that the goal of aim 1 was achieved. Our nanoemulsion system has proved to be successful in all the aspects including stability, drug loading, drug dispersion, and drug release.

In the in-vitro activity and brain delivery capability part, our nanoemulsion systems have been proved to be safe to human cells through viability studies in different cell lines. No organic solvent residual was detected. Cell update and drug transport studies confirmed the brain delivery ability of Tf-NE-DRV. Surprisingly with a large amount of DHA in the

system, NE-DRV was also able to achieve decent brain delivery without the help of transferrin. So, we explored more on the mechanism of NE-DRV brain delivery. In conclusion, the DHA can better solubilize and transport the drug. We used plasmid to successfully create a lentiviral infected cell model for efficacy study. Tf-NE-DRV was proved has the same anti-viral activity as the free drug darunavir.

Both NE-DRV and Tf-NE-DRV can successfully enter the brain in vivo. The biodistribution data also revealed that the brain drug concentration was significantly increased to reach the IC50 of darunavir which is about 5nM after 2-day consecutive dosing. Furthermore, the drug concentration can maintain for day 3. But for the free drug group, the drug concentration was decreased for day 3. Because darunavir is the substrate of P-glycoprotein receptor and it can't retain inside the brain. All these results proved our formulation is superior to the free form of the drug. Although liver and spleen retained most of the drugs, which indicates there is still room for stability improvement.

5.5. Future directions

Even though we successfully achieved all the goals of this project, there are still a few issues that need to be addressed in order to achieve a successful in vivo brain targeting nanoemulsion formulation. The following part is dedicated to some future works to make the system more clinically adaptable.

5.5.1. Formulation optimization

In vivo stability should be optimized by testing different lipid ratios and oil, drug ratios for the formulation. This part of the work is not entirely fulfilled in this project. With the improvement of formulation stability, we can foresee better in vivo therapeutic function of this formulation.

Without the help of transferrin targeting, NE-DRV can achieve relatively same results as Tf-NE-DRV. We may put more effort to investigate plain DHA nanoemulsion formulations for brain targeting delivery. The manufacturing process can be significantly simplified if omitting the targeting moiety conjugation step.

5.5.2. Co-delivery of therapeutic agents

Cocktail therapy is the standard treatment for HIV patients. Although darunavir has a very high barrier to resistance. It is better to co-deliver antiretroviral therapies to prevent resistance and achieve the best therapeutic outcomes.

5.5.3. Further efficacy studies

We overdosed during the efficacy studies. To further investigate the efficacy of Tf-NE-DRV, we should generate a dose-response curve. Potentially nanoemulsion formulation may have better therapeutic results since the carrier can deliver more therapeutic agents into target cells.

We used the 293T cell line to develop the model which is not the most representative one. We should develop a diseased CNS cell model. For example, the microglial cell line will be a better choice for further efficacy study.

5.5.4. In vivo studies

Further in vivo studies were necessary to investigate the therapeutic activity of Tf-NE-DRV. CNS infected animal model needs to be developed to investigate the in-vivo antiviral activity of Tf-NE-DRV.

BIBLIOGRAPHY

1. Ricci, M.; Blasi, P.; Giovagnoli, S.; Rossi, C., Delivering drugs to the central nervous system: a medicinal chemistry or a pharmaceutical technology issue? *Curr Med Chem* **2006,** *13* (15), 1757-75.

2. K, B.; P, C., Lipid nano particulate drug delivery: An overview of the emerging trend. *The Pharma Innovation Journal* **2018,** *7* (7), 10.

3. Garcia-Garcia, E.; Andrieux, K.; Gil, S.; Couvreur, P., Colloidal carriers and blood-brain barrier (BBB) translocation: a way to deliver drugs to the brain? *Int J Pharm* **2005,** *298* (2), 274-92.

4. Zhao, M.; Chang, J.; Fu, X.; Liang, C.; Liang, S.; Yan, R.; Li, A., Nano-sized cationic polymeric magnetic liposomes significantly improves drug delivery to the brain in rats. *J Drug Target* **2012,** *20* (5), 416-21.

5. Lipinski, C. A.; Lombardo, F.; Dominy, B. W.; Feeney, P. J., Experimental and computational approaches to estimate solubility and permeability in drug discovery and development settings. *Adv Drug Deliv Rev* **2001,** *46* (1-3), 3-26.

6. Visser, C. C.; Stevanović, S.; Voorwinden, L. H.; van Bloois, L.; Gaillard, P. J.; Danhof, M.; Crommelin, D. J.; de Boer, A. G., Targeting liposomes with protein drugs to the blood-brain barrier in vitro. *Eur J Pharm Sci* **2005,** *25* (2-3), 299-305.

7. Allémann, E.; Leroux, J. C.; Gurny, R.; Doelker, E., In vitro extended-release properties of drug-loaded poly(DL-lactic acid) nanoparticles produced by a salting-out procedure. *Pharm Res* **1993,** *10* (12), 1732-7.

8. Betancor, L.; Luckarift, H. R., Bioinspired enzyme encapsulation for biocatalysis. *Trends Biotechnol* **2008,** *26* (10), 566-72.

9. Cheng, Y.; Wang, J.; Rao, T.; He, X.; Xu, T., Pharmaceutical applications of dendrimers: promising nanocarriers for drug delivery. *Front Biosci* **2008,** *13*, 1447-71.

10. Kaur, I. P.; Bhandari, R.; Bhandari, S.; Kakkar, V., Potential of solid lipid nanoparticles in brain targeting. *J Control Release* **2008,** *127* (2), 97-109.

11. Barbu, E.; Molnàr, E.; Tsibouklis, J.; Górecki, D. C., The potential for nanoparticle-based drug delivery to the brain: overcoming the blood-brain barrier. *Expert Opin Drug Deliv* **2009,** *6* (6), 553-65.

12. Soni, S.; Ruhela, R. K.; Medhi, B., Nanomedicine in Central Nervous System (CNS) Disorders: A Present and Future Prospective. *Adv Pharm Bull* **2016,** *6* (3), 319-335.

13. Costantino, L.; Boraschi, D., Is there a clinical future for polymeric nanoparticles as brain-targeting drug delivery agents? *Drug Discov Today* **2012,** *17* (7-8), 367-78.

14. Béduneau, A.; Saulnier, P.; Benoit, J. P., Active targeting of brain tumors using nanocarriers. *Biomaterials* **2007,** *28* (33), 4947-67.

15. Faraji, A. H.; Wipf, P., Nanoparticles in cellular drug delivery. *Bioorg Med Chem* **2009,** *17* (8), 2950-62.

16. Banks, W. A.; Kastin, A. J.; Barrera, C. M., Delivering peptides to the central nervous system: dilemmas and strategies. *Pharm Res* **1991,** *8* (11), 1345-50.

17. Roney, C.; Kulkarni, P.; Arora, V.; Antich, P.; Bonte, F.; Wu, A.; Mallikarjuana, N. N.; Manohar, S.; Liang, H. F.; Kulkarni, A. R.; Sung, H. W.; Sairam, M.; Aminabhavi, T. M., Targeted nanoparticles for drug delivery through the blood-brain barrier for Alzheimer's disease. *J Control Release* **2005,** *108* (2-3), 193-214.

18. Bronich, T. K.; Bontha, S.; Shlyakhtenko, L. S.; Bromberg, L.; Hatton, T. A.; Kabanov, A. V., Template-assisted synthesis of nanogels from Pluronic-modified poly(acrylic acid). *J Drug Target* **2006,** *14* (6), 357-66.

19. Ahn, J.; Miura, Y.; Yamada, N.; Chida, T.; Liu, X.; Kim, A.; Sato, R.; Tsumura, R.; Koga, Y.; Yasunaga, M.; Nishiyama, N.; Matsumura, Y.; Cabral, H.; Kataoka, K., Antibody fragment-conjugated polymeric micelles incorporating platinum drugs for targeted therapy of pancreatic cancer. *Biomaterials* **2015,** *39*, 23-30.

20. Jain, S. K.; Gupta, Y.; Ramalingam, L.; Jain, A.; Khare, P.; Bhargava, D., Lactose-Conjugated PLGA Nanoparticles for Enhanced Delivery of Rifampicin to the Lung for Effective Treatment of Pulmonary Tuberculosis. *PDA J Pharm Sci Technol* **2010,** *64* (3), 278-87.

21. Mohamed, S.; Parayath, N. N.; Taurin, S.; Greish, K., Polymeric nano-micelles: versatile platform for targeted delivery in cancer. *Ther Deliv* **2014,** *5* (10), 1101-21.

22. Sultan, B.; Fatma, G. I.; Huseyin, E.; Nurettin, S., One-step fabrication of biocompatible carboxymethyl cellulose polymeric particles for drug delivery systems. *Carbohydrate Polymers* **2011,** *86* (2), 8.

23. Akimoto, J.; Nakayama, M.; Okano, T., Temperature-responsive polymeric micelles for optimizing drug targeting to solid tumors. *J Control Release* **2014,** *193*, 2-8.

24. Zhao, B. X.; Zhao, Y.; Huang, Y.; Luo, L. M.; Song, P.; Wang, X.; Chen, S.; Yu, K. F.; Zhang, X.; Zhang, Q., The efficiency of tumor-specific pH-responsive peptide-modified polymeric micelles containing paclitaxel. *Biomaterials* **2012,** *33* (8), 2508-20.

25. Tadros, T.; Izquierdo, P.; Esquena, J.; Solans, C., Formation and stability of nano-emulsions. *Adv Colloid Interface Sci* **2004,** *108-109,* 303-18.

26. Fryd, M. M.; Mason, T. G., Nanoinclusions in cryogenically quenched nanoemulsions. *Langmuir* **2012,** *28* (33), 12015-21.

27. P., I.; J., E.; F., T. T., **2002**.

28. Koroleva, M. Y.; Yurtov, E. V. e., Nanoemulsions: the properties, methods of preparation and promising applications. *Russian Chemical Reviews* **2012,** *81* (1), 21-43.

29. Anton, N.; Benoit, J.-P.; Saulnier, P., Design and production of nanoparticles formulated from nano-emulsion templates—a review. *Journal of Controlled Release* **2008,** *128* (3), 185-199.

30. Feng, J.; Roche, M.; Vigolo, D.; Arnaudov, L. N.; Stoyanov, S. D.; Gurkov, T. D.; Tsutsumanova, G. G.; Stone, H. A., **Nanoemulsions obtained via bubble bursting at a compound interface**. *Nature physics* **2014,** *10,* 6.

31. Fryd, M. M.; Mason, T. G., Time-dependent nanoemulsion droplet size reduction by evaporative ripening. *The Journal of Physical Chemistry Letters* **2010,** *1* (23), 3349-3353.

32. Jaiswal, M.; Dudhe, R.; Sharma, P., Nanoemulsion: an advanced mode of drug delivery system. *3 Biotech* **2015,** *5* (2), 123-127.

33. Setya, S.; Talegaonkar, S.; Razdan, B., Nanoemulsions: formulation methods and stability aspects. *World J. Pharm. Pharm. Sci* **2014,** *3* (2), 2214-2228.

34. Leong, T.; Wooster, T.; Kentish, S.; Ashokkumar, M., Minimising oil droplet size using ultrasonic emulsification. *Ultrasonics Sonochemistry* **2009,** *16* (6), 721-727.

35. Gaikwad, S. G.; Pandit, A. B., Ultrasound emulsification: effect of ultrasonic and physicochemical properties on dispersed phase volume and droplet size. *Ultrasonics sonochemistry* **2008,** *15* (4), 554-563.

36. Chime, S.; Kenechukwu, F.; Attama, A., Nanoemulsions—advances in formulation, characterization and applications in drug delivery. In *Application of nanotechnology in drug delivery*, InTech: 2014.

37. (HHS), D. o. H. a. H. S. " What Are HIV and AIDS?".

38. Mandell, G.; Bennett, J.; Dolin, R., In *Mandell, Douglas, and Bennett's Principles and Practice of Infectious Diseases*, 2010.

39. Rao, K. S.; Ghorpade, A.; Labhasetwar, V., Targeting anti-HIV drugs to the CNS. *Expert Opin Drug Deliv* **2009,** *6* (8), 771-84.

40. Nath, A., Neurologic complications of human immunodeficiency virus infection. *Continuum: Lifelong Learning in Neurology* **2015,** *21* (6, Neuroinfectious Disease), 1557-1576.

41. McArthur, J.; Smith, B., Neurologic complications and considerations in HIV-infected persons. *Current infectious disease reports* **2013,** *15* (1), 61-66.

42. Navia, B. A.; Jordan, B. D.; Price, R. W., The AIDS dementia complex: I. clinical features. *Annals of Neurology* **1986,** *19* (6).

43. Arendt, G.; Hefter, H.; Hoemberg, V.; Nelles, H. W.; Elsing, C.; Freund, H. J., Early abnormalities of cognitive event-related potentials in HIV-infected patients without clinically evident CNS deficits. *Electroencephalogr Clin Neurophysiol Suppl* **1990,** *41*, 370-80.

44. Antinori, A.; Arendt, G.; Becker, J. T.; Brew, B. J.; Byrd, D. A.; Cherner, M.; Clifford, D. B.; Cinque, P.; Epstein, L. G.; Goodkin, K.; Gisslen, M.; Grant, I.; Heaton, R. K.; Joseph, J.; Marder, K.; Marra, C. M.; McArthur, J. C.; Nunn, M.; Price, R. W.; Pulliam, L.; Robertson, K. R.; Sacktor, N.; Valcour, V.; Wojna, V. E., Updated research nosology for HIV-associated neurocognitive disorders. *Neurology* **2007,** *69* (18), 1789-99.

45. Crum-Cianflone, N. F.; Moore, D. J.; Letendre, S.; Poehlman Roediger, M.; Eberly, L.; Weintrob, A.; Ganesan, A.; Johnson, E.; Del Rosario, R.; Agan, B. K.; Hale, B. R., Low prevalence of neurocognitive impairment in early diagnosed and managed HIV-infected persons. *Neurology* **2013,** *80* (4), 371-9.

46. Sevigny, J. J.; Albert, S. M.; McDermott, M. P.; Schifitto, G.; McArthur, J. C.; Sacktor, N.; Conant, K.; Selnes, O. A.; Stern, Y.; McClernon, D. R.; Palumbo, D.; Kieburtz, K.; Riggs, G.; Cohen, B.; Marder, K.; Epstein, L. G., An evaluation of neurocognitive status and markers of immune activation as predictors of time to death in advanced HIV infection. *Arch Neurol* **2007,** *64* (1), 97-102.

47. Gary, F.; Concordet, D.; Berland, H. M.; Berthelot, X.; Darré, R., Does the 1/29 Robertsonian translocation affect the fertility of Blonde d'Aquitaine breed bulls? *Theriogenology* **1991,** *36* (3), 419-25.

48. Elovaara, I.; Seppälä, I.; Poutiainen, E.; Suni, J.; Valle, S. L., Intrathecal humoral immunologic response in neurologically symptomatic and asymptomatic patients with human immunodeficiency virus infection. *Neurology* **1988,** *38* (9), 1451-6.

49. Marra, C. M.; Maxwell, C. L.; Collier, A. C.; Robertson, K. R.; Imrie, A., Interpreting cerebrospinal fluid pleocytosis in HIV in the era of potent antiretroviral therapy. *BMC Infect Dis* **2007,** *7*, 37.

50. Neuen-Jacob, E., Neurotransmitter Effects in Human Immunodeficiency Virus (HIV) and Simian Immuno-Deficiency Virus (SIV) Infection. *Anti-Inflammatory & Anti-Allergy Agents in Medicinal Chemistry* **2009,** *8* (2), 11.

51. Shaw, G. M.; Harper, M. E.; Hahn, B. H.; Epstein, L. G.; Gajdusek, D. C.; Price, R. W.; Navia, B. A.; Petito, C. K.; O'Hara, C. J.; Groopman, J. E., HTLV-III infection in brains of children and adults with AIDS encephalopathy. *Science* **1985,** *227* (4683), 177-82.

52. Everall, I. P.; Heaton, R. K.; Marcotte, T. D.; Ellis, R. J.; McCutchan, J. A.; Atkinson, J. H.; Grant, I.; Mallory, M.; Masliah, E., Cortical synaptic density is reduced in mild to moderate human immunodeficiency virus neurocognitive disorder. HNRC Group. HIV Neurobehavioral Research Center. *Brain Pathol* **1999,** *9* (2), 209-17.

53. Silva, K.; Hope-Lucas, C.; White, T.; Hairston, T. K.; Rameau, T.; Brown, A., Cortical neurons are a prominent source of the proinflammatory cytokine osteopontin in HIV-associated neurocognitive disorders. *J Neurovirol* **2015,** *21* (2), 174-85.

54. Desplats, P.; Dumaop, W.; Smith, D.; Adame, A.; Everall, I.; Letendre, S.; Ellis, R.; Cherner, M.; Grant, I.; Masliah, E., Molecular and pathologic insights from latent HIV-1 infection in the human brain. *Neurology* **2013,** *80* (15), 1415-23.

55. Levine, A. J.; Soontornniyomkij, V.; Achim, C. L.; Masliah, E.; Gelman, B. B.; Sinsheimer, J. S.; Singer, E. J.; Moore, D. J., Multilevel analysis of

neuropathogenesis of neurocognitive impairment in HIV. *J Neurovirol* **2016,** *22* (4), 431-41.

56. Cherner, M.; Masliah, E.; Ellis, R. J.; Marcotte, T. D.; Moore, D. J.; Grant, I.; Heaton, R. K., Neurocognitive dysfunction predicts postmortem findings of HIV encephalitis. *Neurology* **2002,** *59* (10), 1563-7.

57. Glass, J. D.; Fedor, H.; Wesselingh, S. L.; McArthur, J. C., Immunocytochemical quantitation of human immunodeficiency virus in the brain: correlations with dementia. *Ann Neurol* **1995,** *38* (5), 755-62.

58. Ellis, R. J.; Moore, D. J.; Childers, M. E.; Letendre, S.; McCutchan, J. A.; Wolfson, T.; Spector, S. A.; Hsia, K.; Heaton, R. K.; Grant, I., Progression to neuropsychological impairment in human immunodeficiency virus infection predicted by elevated cerebrospinal fluid levels of human immunodeficiency virus RNA. *Arch Neurol* **2002,** *59* (6), 923-8.

59. Heaton, R. K.; Franklin, D. R.; Ellis, R. J.; McCutchan, J. A.; Letendre, S. L.; Leblanc, S.; Corkran, S. H.; Duarte, N. A.; Clifford, D. B.; Woods, S. P.; Collier, A. C.; Marra, C. M.; Morgello, S.; Mindt, M. R.; Taylor, M. J.; Marcotte, T. D.; Atkinson, J. H.; Wolfson, T.; Gelman, B. B.; McArthur, J. C.; Simpson, D. M.; Abramson, I.; Gamst, A.; Fennema-Notestine, C.; Jernigan, T. L.; Wong, J.; Grant, I.; Group, C.; Group, H., HIV-associated neurocognitive disorders before and during the era of combination antiretroviral therapy: differences in rates, nature, and predictors. *J Neurovirol* **2011,** *17* (1), 3-16.

60. Navia, B. A.; Cho, E.; Petito, C. K.; Price, R. W., The AIDS dementia complex: II. Neuropathology. *Annals of Neurology* **1986,** *19* (6), 11.

61. Booss, J.; Harris, S. A., Neurology of AIDS virus infection: a clinical classification. *Yale J Biol Med* **1987,** *60* (6), 537-43.

62. Chan, L. G.; Wong, C. S., HIV-Associated Neurocognitive Disorders--An issue of Growing Importance. *Ann Acad Med Singapore* **2013,** *42* (10), 527-34.

63. Sacktor, N., The epidemiology of human immunodeficiency virus–associated neurological disease in the era of highly active antiretroviral therapy. *Journal of neurovirology* **2002,** *8*.

64. Eggers, C. C.; van Lunzen, J.; Buhk, T.; Stellbrink, H. J., HIV infection of the central nervous system is characterized by rapid turnover of viral RNA in cerebrospinal fluid. *J Acquir Immune Defic Syndr Hum Retrovirol* **1999,** *20* (3), 259-64.

65. Eggers, C.; Stuerenburg, H. J.; Schafft, T.; Zöllner, B.; Feucht, H. H.; Stellbrink, H. J.; van Lunzen, J., Rapid clearance of human immunodeficiency virus type 1 from ventricular cerebrospinal fluid during antiretroviral treatment. *Ann Neurol* **2000,** *47* (6), 816-9.

66. Evers, S.; Grotemeyer, K. H.; Reichelt, D.; Lüttmann, S.; Husstedt, I. W., Impact of antiretroviral treatment on AIDS dementia: a longitudinal prospective event-related potential study. *J Acquir Immune Defic Syndr Hum Retrovirol* **1998,** *17* (2), 143-8.

67. Sidtis, J. J.; Gatsonis, C.; Price, R. W.; Singer, E. J.; Collier, A. C.; Richman, D. D.; Hirsch, M. S.; Schaerf, F. W.; Fischl, M. A.; Kieburtz, K., Zidovudine treatment of the AIDS dementia complex: results of a placebo-controlled trial. AIDS Clinical Trials Group. *Ann Neurol* **1993,** *33* (4), 343-9.

68. Cysique, L. A.; Vaida, F.; Letendre, S.; Gibson, S.; Cherner, M.; Woods, S. P.; McCutchan, J. A.; Heaton, R. K.; Ellis, R. J., Dynamics of cognitive change in

impaired HIV-positive patients initiating antiretroviral therapy. *Neurology* **2009,** *73* (5), 342-8.

69. Heaton, R. K.; Clifford, D. B.; Franklin, D. R.; Woods, S. P.; Ake, C.; Vaida, F.; Ellis, R. J.; Letendre, S. L.; Marcotte, T. D.; Atkinson, J. H.; Rivera-Mindt, M.; Vigil, O. R.; Taylor, M. J.; Collier, A. C.; Marra, C. M.; Gelman, B. B.; McArthur, J. C.; Morgello, S.; Simpson, D. M.; McCutchan, J. A.; Abramson, I.; Gamst, A.; Fennema-Notestine, C.; Jernigan, T. L.; Wong, J.; Grant, I.; Group, C., HIV-associated neurocognitive disorders persist in the era of potent antiretroviral therapy: CHARTER Study. *Neurology* **2010,** *75* (23), 2087-96.

70. Letendre, J.; Barrieras, D.; Franc-Guimond, J.; Abdo, A.; Houle, A. M., Topical triamcinolone for persistent phimosis. *J Urol* **2009,** *182* (4 Suppl), 1759-63.

71. Letendre, S., Central nervous system complications in HIV disease: HIV-associated neurocognitive disorder. *Top Antivir Med* **2011,** *19* (4), 137-42.

72. Cusini, A.; Vernazza, P. L.; Yerly, S.; Decosterd, L. A.; Ledergerber, B.; Fux, C. A.; Rohrbach, J.; Widmer, N.; Hirschel, B.; Gaudenz, R.; Cavassini, M.; Klimkait, T.; Zenger, F.; Gutmann, C.; Opravil, M.; Günthard, H. F.; Study, S. H. C., Higher CNS penetration-effectiveness of long-term combination antiretroviral therapy is associated with better HIV-1 viral suppression in cerebrospinal fluid. *J Acquir Immune Defic Syndr* **2013,** *62* (1), 28-35.

73. Cysique, L. A.; Waters, E. K.; Brew, B. J., Central nervous system antiretroviral efficacy in HIV infection: a qualitative and quantitative review and implications for future research. *BMC Neurol* **2011,** *11*, 148.

74. Letendre, S.; Marquie-Beck, J.; Capparelli, E.; Best, B.; Clifford, D.; Collier, A. C.; Gelman, B. B.; McArthur, J. C.; McCutchan, J. A.; Morgello, S.; Simpson, D.; Grant, I.; Ellis, R. J.; Group, C., Validation of the CNS Penetration-Effectiveness rank for quantifying antiretroviral penetration into the central nervous system. *Arch Neurol* **2008,** *65* (1), 65-70.

75. Abbott, N. J.; Patabendige, A. A.; Dolman, D. E.; Yusof, S. R.; Begley, D. J., Structure and function of the blood-brain barrier. *Neurobiol Dis* **2010,** *37* (1), 13-25.

76. Abbott, N. J., Blood-brain barrier structure and function and the challenges for CNS drug delivery. *J Inherit Metab Dis* **2013,** *36* (3), 437-49.

77. Sagar, V.; Pilakka-Kanthikeel, S.; Pottathil, R.; Saxena, S. K.; Nair, M., Towards nanomedicines for neuroAIDS. *Rev Med Virol* **2014,** *24* (2), 103-24.

78. Tajes, M.; Ramos-Fernández, E.; Weng-Jiang, X.; Bosch-Morató, M.; Guivernau, B.; Eraso-Pichot, A.; Salvador, B.; Fernàndez-Busquets, X.; Roquer, J.; Muñoz, F. J., The blood-brain barrier: structure, function and therapeutic approaches to cross it. *Mol Membr Biol* **2014,** *31* (5), 152-67.

79. Takasawa, K.; Terasaki, T.; Suzuki, H.; Sugiyama, Y., In vivo evidence for carrier-mediated efflux transport of 3'-azido-3'-deoxythymidine and 2',3'-dideoxyinosine across the blood-brain barrier via a probenecid-sensitive transport system. *J Pharmacol Exp Ther* **1997,** *281* (1), 369-75.

80. Wang, Y.; Sawchuk, R. J., Zidovudine transport in the rabbit brain during intravenous and intracerebroventricular infusion. *J Pharm Sci* **1995,** *84* (7), 871-6.

81. Enting, R. H.; Hoetelmans, R. M.; Lange, J. M.; Burger, D. M.; Beijnen, J. H.; Portegies, P., Antiretroviral drugs and the central nervous system. *AIDS* **1998,** *12* (15), 1941-55.

82. Bagasra, O., A unified concept of HIV latency. *Expert Opin Biol Ther* **2006,** *6* (11), 1135-49.

83. Stockwell, J.; Abdi, N.; Lu, X.; Maheshwari, O.; Taghibiglou, C., Novel central nervous system drug delivery systems. *Chem Biol Drug Des* **2014,** *83* (5), 507-20.

84. Fortin, D.; Gendron, C.; Boudrias, M.; Garant, M. P., Enhanced chemotherapy delivery by intraarterial infusion and blood-brain barrier disruption in the treatment of cerebral metastasis. *Cancer* **2007,** *109* (4), 751-60.

85. Hynynen, K., Ultrasound for drug and gene delivery to the brain. *Adv Drug Deliv Rev* **2008,** *60* (10), 1209-17.

86. Hynynen, K.; Pomeroy, O.; Smith, D. N.; Huber, P. E.; McDannold, N. J.; Kettenbach, J.; Baum, J.; Singer, S.; Jolesz, F. A., MR imaging-guided focused ultrasound surgery of fibroadenomas in the breast: a feasibility study. *Radiology* **2001,** *219* (1), 176-85.

87. Treat, L. H.; McDannold, N.; Vykhodtseva, N.; Zhang, Y.; Tam, K.; Hynynen, K., Targeted delivery of doxorubicin to the rat brain at therapeutic levels using MRI-guided focused ultrasound. *Int J Cancer* **2007,** *121* (4), 901-7.

88. Tam, V. H.; Sosa, C.; Liu, R.; Yao, N.; Priestley, R. D., Nanomedicine as a non-invasive strategy for drug delivery across the blood brain barrier. *Int J Pharm* **2016,** *515* (1-2), 331-342.

89. Downs, M. E.; Buch, A.; Karakatsani, M. E.; Konofagou, E. E.; Ferrera, V. P., Blood-Brain Barrier Opening in Behaving Non-Human Primates via Focused Ultrasound with Systemically Administered Microbubbles. *Sci Rep* **2015,** *5*, 15076.

90. Gabathuler, R., Approaches to transport therapeutic drugs across the blood-brain barrier to treat brain diseases. *Neurobiol Dis* **2010,** *37* (1), 48-57.

91. Pardridge, W. M., Drug targeting to the brain. *Pharm Res* **2007,** *24* (9), 1733-44.

92. Rautio, J.; Laine, K.; Gynther, M.; Savolainen, J., Prodrug approaches for CNS delivery. *AAPS J* **2008,** *10* (1), 92-102.

93. Misra, A.; Ganesh, S.; Shahiwala, A.; Shah, S. P., Drug delivery to the central nervous system: a review. *J Pharm Pharm Sci* **2003,** *6* (2), 252-73.

94. Guastella, A. J.; Einfeld, S. L.; Gray, K. M.; Rinehart, N. J.; Tonge, B. J.; Lambert, T. J.; Hickie, I. B., Intranasal oxytocin improves emotion recognition for youth with autism spectrum disorders. *Biol Psychiatry* **2010,** *67* (7), 692-4.

95. Shingaki, T.; Inoue, D.; Furubayashi, T.; Sakane, T.; Katsumi, H.; Yamamoto, A.; Yamashita, S., Transnasal delivery of methotrexate to brain tumors in rats: a new strategy for brain tumor chemotherapy. *Mol Pharm* **2010,** *7* (5), 1561-8.

96. Ojewole, E.; Mackraj, I.; Naidoo, P.; Govender, T., Exploring the use of novel drug delivery systems for antiretroviral drugs. *Eur J Pharm Biopharm* **2008,** *70* (3), 697-710.

97. Kreuter, J., Nanoparticulate systems for brain delivery of drugs. *Adv Drug Deliv Rev* **2001,** *47* (1), 65-81.

98. Johnsen, K. B.; Moos, T., Revisiting nanoparticle technology for blood-brain barrier transport: Unfolding at the endothelial gate improves the fate of transferrin receptor-targeted liposomes. *J Control Release* **2016,** *222*, 32-46.

99. Gao, K.; Jiang, X., Influence of particle size on transport of methotrexate across blood brain barrier by polysorbate 80-coated polybutylcyanoacrylate nanoparticles. *Int J Pharm* **2006,** *310* (1-2), 213-9.

100. Letchford, K.; Burt, H., A review of the formation and classification of amphiphilic block copolymer nanoparticulate structures: micelles, nanospheres, nanocapsules and polymersomes. *Eur J Pharm Biopharm* **2007,** *65* (3), 259-69.

101. Sharma, G.; Lakkadwala, S.; Modgil, A.; Singh, J., The Role of Cell-Penetrating Peptide and Transferrin on Enhanced Delivery of Drug to Brain. *Int J Mol Sci* **2016,** *17* (6).

102. Chen, Y.; Liu, L., Modern methods for delivery of drugs across the blood-brain barrier. *Adv Drug Deliv Rev* **2012,** *64* (7), 640-65.

103. Mora, M.; Sagristá, M. L.; Trombetta, D.; Bonina, F. P.; De Pasquale, A.; Saija, A., Design and characterization of liposomes containing long-chain N-acylPEs for brain delivery: penetration of liposomes incorporating GM1 into the rat brain. *Pharm Res* **2002,** *19* (10), 1430-8.

104. Jones, A. R.; Shusta, E. V., Blood-brain barrier transport of therapeutics via receptor-mediation. *Pharm Res* **2007,** *24* (9), 1759-71.

105. Chang, J.; Jallouli, Y.; Kroubi, M.; Yuan, X. B.; Feng, W.; Kang, C. S.; Pu, P. Y.; Betbeder, D., Characterization of endocytosis of transferrin-coated PLGA nanoparticles by the blood-brain barrier. *Int J Pharm* **2009,** *379* (2), 285-92.

106. Xie, H.; Zhu, Y.; Jiang, W.; Zhou, Q.; Yang, H.; Gu, N.; Zhang, Y.; Xu, H.; Yang, X., Lactoferrin-conjugated superparamagnetic iron oxide nanoparticles as a specific MRI contrast agent for detection of brain glioma in vivo. *Biomaterials* **2011,** *32* (2), 495-502.

107. Georgieva, J. V.; Hoekstra, D.; Zuhorn, I. S., Smuggling Drugs into the Brain: An Overview of Ligands Targeting Transcytosis for Drug Delivery across the Blood-Brain Barrier. *Pharmaceutics* **2014,** *6* (4), 557-83.

108. Tortorella, S.; Karagiannis, T. C., Transferrin receptor-mediated endocytosis: a useful target for cancer therapy. *J Membr Biol* **2014,** *247* (4), 291-307.

109. Kumagai, A. K.; Eisenberg, J. B.; Pardridge, W. M., Absorptive-mediated endocytosis of cationized albumin and a beta-endorphin-cationized albumin chimeric peptide by isolated brain capillaries. Model system of blood-brain barrier transport. *J Biol Chem* **1987,** *262* (31), 15214-9.

110. Schwarze, S. R.; Ho, A.; Vocero-Akbani, A.; Dowdy, S. F., In vivo protein transduction: delivery of a biologically active protein into the mouse. *Science* **1999,** *285* (5433), 1569-72.

111. Allhenn, D.; Boushehri, M. A.; Lamprecht, A., Drug delivery strategies for the treatment of malignant gliomas. *Int J Pharm* **2012,** *436* (1-2), 299-310.

112. Singh, Y.; Meher, J. G.; Raval, K.; Khan, F. A.; Chaurasia, M.; Jain, N. K.; Chourasia, M. K., Nanoemulsion: Concepts, development and applications in drug delivery. *J Control Release* **2017,** *252,* 28-49.

113. Gupta, A.; Eral, H. B.; Hatton, T. A.; Doyle, P. S., Nanoemulsions: formation, properties and applications. *Soft Matter* **2016,** *12* (11), 2826-41.

114. Wellner, N.; Diep, T. A.; Janfelt, C.; Hansen, H. S., N-acylation of phosphatidylethanolamine and its biological functions in mammals. *Biochim Biophys Acta* **2013,** *1831* (3), 652-62.

115. Araujo, L.; Löbenberg, R.; Kreuter, J., Influence of the surfactant concentration on the body distribution of nanoparticles. *J Drug Target* **1999,** *6* (5), 373-85.

116. Labhasetwar, V.; Song, C.; Humphrey, W.; Shebuski, R.; Levy, R. J., Arterial uptake of biodegradable nanoparticles: effect of surface modifications. *J Pharm Sci* **1998,** *87* (10), 1229-34.

117. Li, S. D.; Huang, L., Stealth nanoparticles: high density but sheddable PEG is a key for tumor targeting. *J Control Release* **2010,** *145* (3), 178-81.

118. Edwards, R. H., Drug delivery via the blood-brain barrier. *Nat Neurosci* **2001,** *4* (3), 221-2.

119. Gan, C. W.; Feng, S. S., Transferrin-conjugated nanoparticles of poly(lactide)-D-alpha-tocopheryl polyethylene glycol succinate diblock copolymer for targeted drug delivery across the blood-brain barrier. *Biomaterials* **2010,** *31* (30), 7748-57.

120. Jefferies, W. A.; Brandon, M. R.; Hunt, S. V.; Williams, A. F.; Gatter, K. C.; Mason, D. Y., Transferrin receptor on endothelium of brain capillaries. *Nature* **1984,** *312* (5990), 162-3.

121. Sadava D; Hillis DM; Heller HC; MR, B., *Life: The Science of Biology*. Freeman: San Francisco, 2011; p 9.

122. Rizvi, S. A. A.; Saleh, A. M., Applications of nanoparticle systems in drug delivery technology. *Saudi Pharm J* **2018,** *26* (1), 64-70.

123. Ohvo-Rekilä, H.; Ramstedt, B.; Leppimäki, P.; Slotte, J. P., Cholesterol interactions with phospholipids in membranes. *Prog Lipid Res* **2002,** *41* (1), 66-97.

124. Singh, M., Essential fatty acids, DHA and human brain. *Indian J Pediatr* **2005,** *72* (3), 239-42.

125. Zhang, X.; Cao, D.; Li, Y., Nanoparticle hardness controls the internalization pathway for drug delivery. *Nanoscale.* **2015,** *7* (6), 2758-2769.

127. Decosterd, L.; Battegay, M.; Marzolini, C.; Bartels, H., Darunavir concentrations in CSF of HIV-infected individuals when boosted with cobicistat versus ritonavir. *Journal of antimicrobial chemotherapy.* **2017,** *72* (9), 2574-2577.

128. Sosnik, A.; Chiappetta, D. A.; Carcaboso, A. M., Drug delivery systems in HIV pharmacotherapy: what has been done and the challenges standing ahead. *J Control Release* **2009,** *138* (1), 2-15.

129. Back, D.; Sekar, V.; Hoetelmans, R. M., Darunavir: pharmacokinetics and drug interactions. *Antivir Ther* **2008,** *13* (1), 1-13.

130. Ruela Corrêa, J. C.; D'Arcy, D. M.; dos Reis Serra, C. H.; Nunes Salgado, H. R., Darunavir: a critical review of its properties, use and drug interactions. *Pharmacology* **2012,** *90* (1-2), 102-9.

131. Brazel, C. S.; Huang, X.; Brazel, C. S., On the importance and mechanisms of burst release in matrix-controlled drug delivery systems. *Journal of controlled release.* **2001,** *73* (2-3), 121-136.

132. Socha, M.; Lamprecht, A.; El Ghazouani, F.; Sapin, A.; Hasan, A. S.; Ghazouani, F. E.; Hoffman, M.; Maincent, P.; Ubrich, N., Effect of the

microencapsulation of nanoparticles on the reduction of burst release. *International journal of pharmaceutics.* **2007,** *344* (1-2), 53-61.

133. Young, J. A. T.; Frankel, A. D.; Young, J. A. T., HIV-1: Fifteen Proteins and an RNA. *Annual review of biochemistry.* **1998,** *67* (1), 1-25.

134. Weksler, B.; Romero, I. A.; Couraud, P. O., The hCMEC/D3 cell line as a model of the human blood brain barrier. *Fluids Barriers CNS* **2013,** *10* (1), 16.

135. Poller, B.; Gutmann, H.; Krähenbühl, S.; Weksler, B.; Romero, I.; Couraud, P. O.; Tuffin, G.; Drewe, J.; Huwyler, J., The human brain endothelial cell line hCMEC/D3 as a human blood‐brain barrier model for drug transport studies. *Journal of neurochemistry* **2008,** *107* (5), 1358-1368.

136. Hu, X.; Zhou, Z.; Fronczek, F. R.; Couraud, P.-O.; Bhupathiraju, N. V. S. D. K.; Romero, I. A.; Weksler, B.; Vicente, M. G. H., Synthesis and in Vitro Evaluation of BBB Permeability, Tumor Cell Uptake, and Cytotoxicity of a Series of Carboranylporphyrin Conjugates. *Journal of medicinal chemistry.* **2014,** *57* (15), 6718-6728.

137. Horrocks, L. A.; Yeo, Y. K., Health benefits of docosahexaenoic acid (DHA). *Pharmacological research* **1999,** *40* (3), 211-225.

138. Kidd, P. M., Omega-3 DHA and EPA for cognition, behavior, and mood: clinical findings and structural-functional synergies with cell membrane phospholipids. *Alternative medicine review* **2007,** *12* (3), 207.

139. Breckenridge, W.; Gombos, G.; Morgan, I., The lipid composition of adult rat brain synaptosomal plasma membranes. *Biochimica et Biophysica Acta (BBA)-Biomembranes* **1972,** *266* (3), 695-707.

140. Innis, S. M., Dietary (n-3) fatty acids and brain development. *The Journal of nutrition* **2007,** *137* (4), 855-859.

141. Nguyen, L. N.; Ma, D.; Shui, G.; Wong, P.; Cazenave-Gassiot, A.; Zhang, X.; Wenk, M. R.; Goh, E. L.; Silver, D. L., Mfsd2a is a transporter for the essential omega-3 fatty acid docosahexaenoic acid. *Nature* **2014,** *509* (7501), 503.

142. Kampmann, M.; Bassik, M. C.; Kampmann, M., Knocking out the door to tunicamycin entry. *Proceedings of the National Academy of Sciences of the United States of America.* **2011,** *108* (29), 11731-11732.

143. Ben-Zvi, A.; Lacoste, B.; Kur, E.; Andreone, B. J.; Mayshar, Y.; Yan, H.; Gu, C., Mfsd2a is critical for the formation and function of the blood–brain barrier. *Nature* **2014,** *509* (7501), 507.